A Critical Review of the Physicochemical Impacts of Water Chemistry on Shale in Hydraulic Fracturing Systems

Hasan Javed Khan,* Eleanor Spielman-Sun, Adam D. Jew, John Bargar, Anthony Kovscek, and Jennifer L. Druhan*

ABSTRACT: Hydraulic fracturing of unconventional hydrocarbon resources involves the sequential injection of a high-pressure, particle-laden fluid with varying pH's to make commercial production viable in low permeability rocks. This process both requires and produces extraordinary volumes of water. The water used for hydraulic fracturing is typically fresh, whereas "flowback" water is typically saline with a variety of additives which complicate safe disposal. As production operations continue to expand, there is an increasing interest in treating and reusing this high-salinity produced water for further fracturing. Here we review the relevant transport and geochemical properties of shales, and critically analyze the impact of water chemistry (including produced water) on these properties. We discuss five major geochemical mechanisms that are prominently involved in the temporal and spatial evolution of fractures during the stimulation and production phase: shale softening, mineral dissolution, mineral precipitation, fines migration, and wettability alteration. A higher salinity fluid creates both benefits and complications in controlling these mechanisms. For example, higher salinity fluid inhibits clay dispersion, but simultaneously requires more additives to achieve appropriate viscosity for proppant emplacement. In total this review highlights the nuances of enhanced hydrogeochemical shale stimulation in relation to the choice of fracturing fluid chemistry.

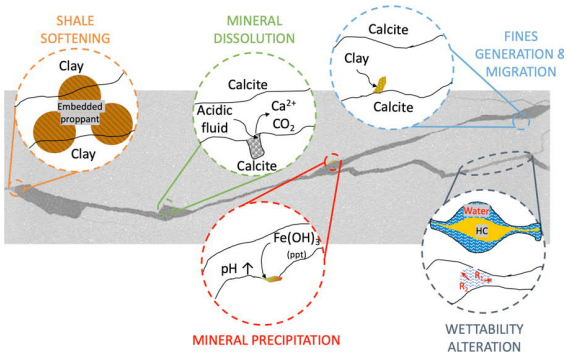

■ INTRODUCTION

The world's total energy consumption is projected to increase 50% by 2050[1] and unconventional oil and gas production is expected to contribute to meeting this demand. Recent technological advancements in these unconventionals have transformed the United States into one of the largest petroleum producers and a net energy exporter[2] for the first time since the 1950s. The majority of unconventional resources are held in highly heterogeneous oil and gas shales, that feature a large variety of (reactive) mineral components and exhibit ultralow permeability.[3−8] These rocks have multimodal porosity and store substantial volumes of hydrocarbons (Table 1) but have low flow potential,[9,10] and need to be stimulated using hydraulic fracturing to make their production economically viable.

Hydraulic fracturing introduces large volumes of high-pressure, water-based fluid (7,000 to 50,000 m^3 per well depending on the shale play[15−18]) to break the rock and generate fluid flow pathways[19,20] (Figure 1). A significant component of this fluid (60−90%[21]) is lost inside the rock, typically within the shale matrix adjacent to the fracture face[21] as a result of both forced and spontaneous imbibition. The remainder is produced at the surface, creating large volumes of

Table 1. Unconventional Resources Are More Widespread but Require Advanced Technology to Extract[a,1,11−14]

gaseous hydrocarbon	
resource	volume (scf)
conventional gas	4.4×10^{11}
coal bed methane	1.1×10^{11}
tight/shale gas	1.6×10^{12}
gas hydrate	5.3×10^{17}
liquid hydrocarbon	
resource	volume (bbl)
conventional oil	4.2×10^{10}
tight/shale oil	1.7×10^{11}
bituminous sands	2.5×10^{11}
oil shales	4.7×10^{12}

[a]Global estimates of the resource in place are colored red and the U.S. estimates are colored blue.

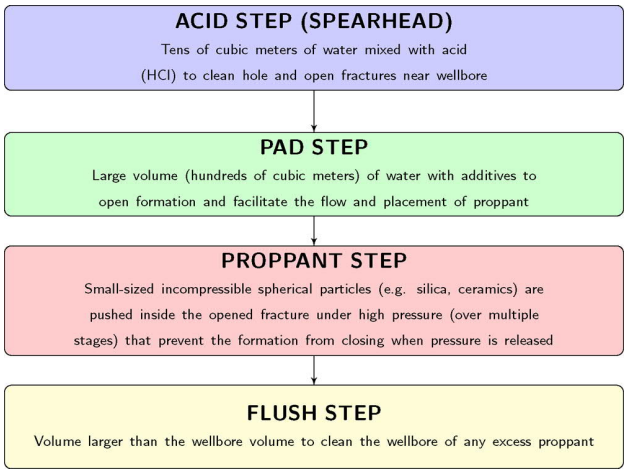

Figure 1. General four-step hydraulic fracturing process. Large volumes of water are consumed during each stage. The injected fluid pH varies from highly acidic (∼−0.3) during the spearhead stage to neutral in the pad stage and slightly alkaline (∼7.5−10) in the proppant stage.

a high-salinity mixture composed of the formation water, as well as the engineered fracturing fluid, that requires costly disposal. This is of particular concern in semiarid regions where freshwater withdrawals for fracture stimulation can amount to a significant portion of total water use within the region.[22,23] Thus, there is a growing interest in the potential to reuse production water for further stimulation.

Water reinjection has seen some success in dry gas plays like the Marcellus where a large percentage of produced water (∼90%[24]) is reused for future stimulations. However, the total volumes of produced water in these plays are much lower than that of unconventional oil plays such as the Permian, which produces ∼15 times more water than the Marcellus.[25] This disparity highlights the fact that the volumes of produced water from shale gas wells vary substantially between plays, ranging from ≤27 m^3 produced water/scm of produced gas in Marcellus to 27−134 m^3/scm in Eagle Ford, Haynesville, and Fayetteville to ≥134 m^3/scm in Barnett shale.[26] The availability of storage sites for this return water can also be a hindrance. For example, only eight class II saltwater disposal sites are available in Pennsylvania.[27] Disposal wells for hydraulic fracturing operations have also raised concerns about induced seismicity.[28,29]

Reusing this "cleaned" produced water for field operations could be of vital importance as the produced volumes can overwhelm the local disposal facilities.[24,30] However, the cleaning necessary to make these fluids suitable for reinjection is nontrivial.[31−34] While conventional oxidation techniques can readily be used to remove organics and some inorganics (e.g., iron) from produced water,[35] monovalent and other divalent inorganic ions can be more difficult and economically burdensome to remove.[36,37] Additionally, such large variation in the produced volumes and salinity add to the complexity of dealing with this fluid from an operational standpoint (e.g., facility size and transport cost).[33,38] These engineered fluids often contain a range of additives designed to control viscosity, friction, microbial growth, and corrosion, resulting in a wide variety of chemical compositions[26,38−41] and contaminants such as oils, soluble organic compounds native to the fractured formation,[42] and degraded products of the injected organic compounds.[43,44] Therefore, injection of this produced water reintroduces the alkali earth metals to the rock and ultimately exacerbates blocking of fractures due to secondary mineral precipitation.[45] Constricted flow can potentially mobilize precipitated mineral scale by matrix dissolution leading to further fracture occlusion.

The result is that, at present, a broad range of water chemistry is being used for the base fluid across hydraulic fracturing operations, some of which have detrimental effects on the production. Thus, it is critical to understand the types and rates of chemical reactions that result from interactions of the various fluid compositions and the diversity of shale reservoirs. If the cleaning procedure could be appropriately optimized, reuse of produced water could provide a benefit or even enhancement to overall production. For example, a recent study[46] has shown that rock permeability can be improved by reinjecting high-salinity fluid, suggesting that a reduction in mobile fines can be achieved by minimizing electrostatic barriers and supporting reattachment to the fracture walls.

Recent reviews[10,17,19,20,24,25,47−51] have considered developments in the individual mechanisms affecting fluid flow pathways by fracturing fluid, tackled the limitations and problems related to the surface facilities when reusing produced water, or focused on the advancements in the water treatment strategies. In what follows we review the literature for shale properties relevant to fluid and solute transport under highly reactive conditions, with emphasis on the impact of water chemistry in driving reactive alterations, and the resulting evolution of fluid flow pathways.

THE HYDRAULIC FRACTURING PROCESS

During unconventional reservoir stimulation, reactivity and transport processes happen simultaneously. These processes impact both the spatial and temporal evolution of the structure of the stimulated volume, including the opening of void space due to solubilization of reactive minerals and the loss of void space due to secondary mineral scaling. All of these processes change the aperture of the fracture and increase or decrease pore dimensions of the matrix and thereby influence access of the fracturing fluid to the shale. In this sense, it is worthwhile to consider a gradient in parameter space: matrix and fracture dissolution and fines release open the flow channel whereas precipitation and fines deposition reduce dimensions of the flow space. This behavior is often encapsulated in dimensionless Péclet (*Pe*) and Damköhler (*Da*) numbers (e.g., Békri et al.[52]), where *Pe* is a ratio of advective to diffusive transport rates and *Da* is a ratio of reaction rate to transport rate. A Damköhler number much greater than 1 implies that the effects of reactivity outpace the effects of transport, implying that as soon as a reactive fluid contacts a surface the reaction occurs rapidly. The system is thus referred to as "transport-limited". During hydraulic fracturing the near wellbore flow rates are large and it is not immediately obvious that transport-control applies. Likewise, *Pe* may be large in the fractured near-well region where advection dominates but very small in the low-permeability matrix. In a heterogeneous system, local values of *Da* and *Pe* may be computed using fracture (μm to mm-scale) and matrix (nm to μm-scale) characteristic length scales, leading to inference of mostly transport-limited conditions in the matrix and reaction-limited conditions in the fractures near the wellbore. These *Da* values are further distinguished by the nature of the reactive pathway to which they are applied. For example, an acidized, anoxic fluid flowing

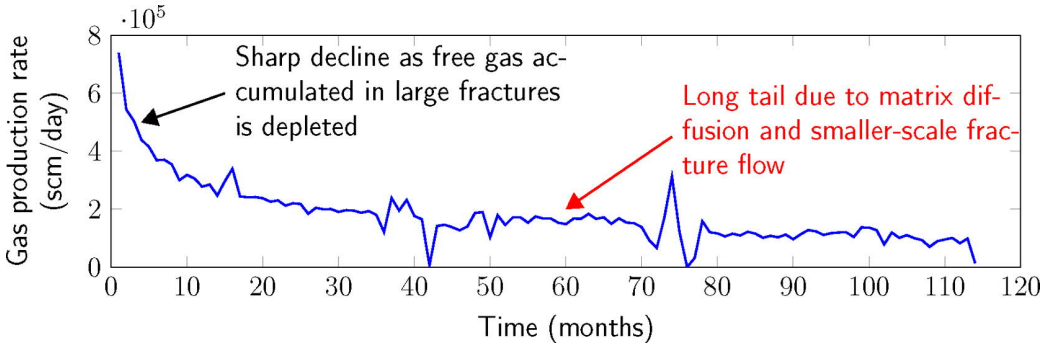

Figure 2. Typical production decline in a well in the Barnett shale (Lease no. 248798, Well no. A10H). Production data available from the Texas Railroad Commission. The sharp initial decline is a result of vacating the gas-filled fractures, with little to no contribution from the shale matrix. Matrix diffusion sustains the low flow rate over long period of time and is dependent on the matrix diffusion coefficient.[65,75]

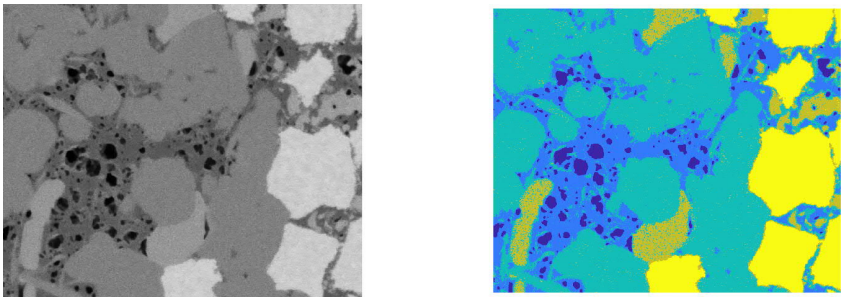

Figure 3. FIB-SEM image of the Vaca Muerta formation at a resolution of 2.5 nm shows pores of multiple sizes. Segmentation shows multiple components including, but not limited to, pore (dark blue), calcite (golden), quartz (teal), organic matter (blue), and pyrite (yellow). Original SEM scan available in ref 90.

through shale would be described by a large value of *Da* associated pH-dependent solubilization, and simultaneously a small value of *Da* associated with oxidative dissolution.

Thus, in natural heterogeneous reservoirs, where it is not intuitively obvious how reactivity and transport are coupled, it is helpful to contextualize the stages of the fracturing process in this dimensionless framework. At present, the majority of shale reactivity studies are conducted under laboratory conditions including batch reaction and flow-through tests of core material.[53−60] A present challenge faced in the field is the linkage of these data to reservoir-scale behavior through such nondimensionalized parametrization. In what follows, we review the steps of the fracturing process, while offering a contextualization of the *Pe* and *Da* associated with each step using local conditions of reactivity and characteristic length.

The first phase of hydraulic fracturing (Figure 1) is comprised of injecting a highly acidic "spearhead" fluid (7.5−15% HCl, pH < 0) intended to clean out the wellbore and dissolve reactive minerals (e.g., carbonates) in the near wellbore region to create pore openings that aid in fracture propagation.[55,61,62] High flow rates with associated small fracture apertures result in $Pe \gg 1$ while the low-pH oxic environment results in extraordinarily high *Da* for reactive minerals. Acid from the initial spearhead is consumed and diluted over the steps of the fracturing operation, reducing its efficacy away from the wellbore, thereby resulting in a decrease in *Da*. As the injected fluid encounters fractures of variable aperture[63] and imbibes into the matrix, the flow rate in the stimulated volume changes and the *Pe* decreases.

A more neutral "pad" fluid (pH ≈ 7) is injected next, at a flow rate ranging from 5 to 16 m^3/min,[19,64] to physically break down the shale formation by cracking the rock, forming an internal connected network, and allowing the acidic spearhead to penetrate deeper inside the reservoir.[48] These high flow rates result in $Pe \gg 1$. The *Da* associated with acid-promoted solubilization varies significantly as the pH changes from highly acidic at the fracture tip to neutral in the wellbore.

Following the pad, slickwater or cross-linked gelled fluids carrying proppant (generally a high-purity well-sorted sand or ceramic) are injected in order to push the proppant as far into the newly formed fractures as possible. Depending on the operator, these injected fluids with proppant packs have a wide range of pH (7.5−10) and viscosity to maximize the transport of the pack into the stimulated rock volume. Following proppant emplacement, the wellbore is flushed to remove the excess proppant. Some wells are put directly on production while some are shut-in for a range of time (generally 3 weeks but it can be upward of months) prior to production to allow hydrocarbons to flow from the rock matrix and accumulate in the fractures. The flow rates associated with this shut-in are only in response to local pressure variations as the system relaxes, suggesting a much lower *Pe*. This accumulation period results in the high hydrocarbon production rate observed in the first year of production[65,66] (Figure 2).

When flowback is initiated, large volumes of relatively low salinity fluid are produced on the surface. With time, the volume of produced water decreases, but the salinity increases (on average ∼7 times higher than seawater[39]) as larger proportions of native formation water come to the surface. Hydrocarbons stored in the large connected pores drain quickly (days to weeks) into the wellbore,[66] resulting in a high initial production rate that sharply declines with time[67] (Figure

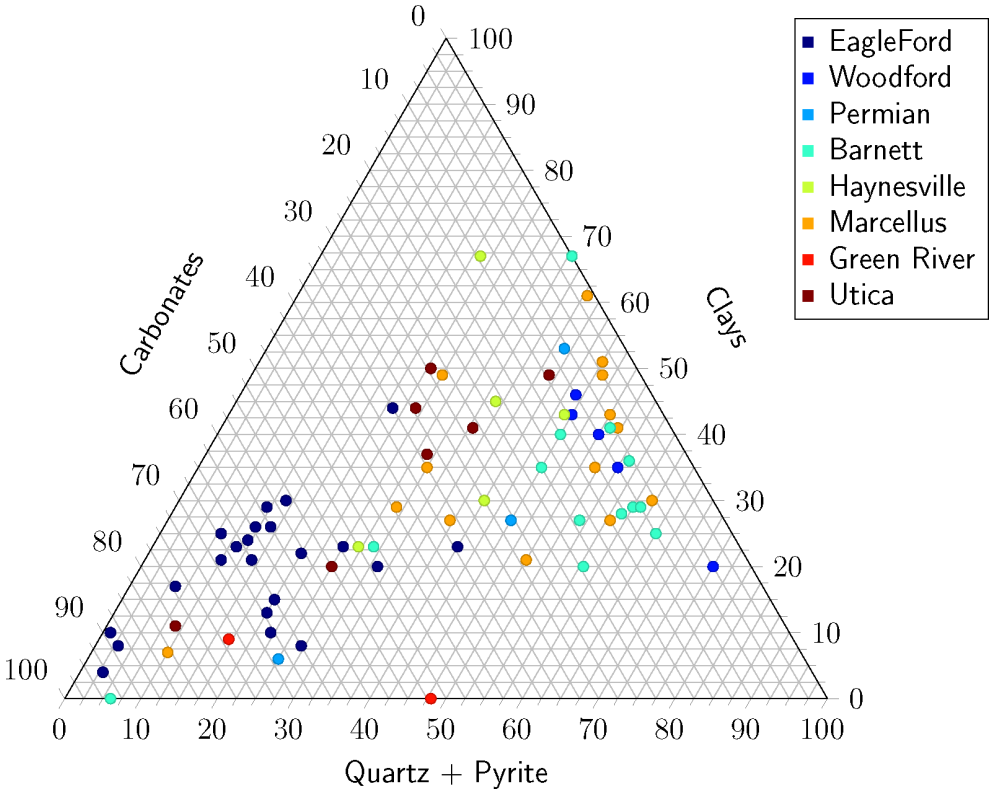

Figure 4. Mineral compositions of shale reservoirs can vary significantly from carbonate-rich to silica-rich resulting in a wide variation of the pore size, porosity, permeability, and mechanical strength.[7,45,69,77,86,91−109]

2). The relatively large hydraulic fractures then maintain the potential for release of the adsorbed oil and gas held within the rock matrix.[9,68,69] With further time (on the order of months to years), hydrocarbon production typically slows along an exponentially declining rate[65,70] (Figure 2). This decline in hydrocarbon production is attributed to a combination of factors including the slow release of the adsorbed gas,[9,71] the collapse of fracture networks,[72,73] and the effects of geochemistry (e.g., accumulation of mineral scaling).[74]

SHALE PETROPHYSICS AND GEOCHEMISTRY

"Shale" is a loosely coined term including, but not limited to, ultrafine-grained rocks such as mudstones, and chalks hosting a variable range of organic matter content and composition. They are primarily composed of clay minerals such as Illite, smectite-montmorillonite, chlorite, and kaolinite, and can also contain a significant proportion of clastic minerals like quartz, feldspar, chert, and carbonates[76] (Figure 3). Organic matter is present at concentrations averaging ∼5% by weight, with individual values as high as 20%.[77] The spatial distribution and density of these minerals dictate the rock mechanical and surface properties,[78] with permeabilities on the order of micro- and nano-Darcy.[49] Detailed studies are usually conducted on individual reservoirs to classify both mineralogy and organic compounds, that are found to vary significantly between different shale plays and even within a specific play,[79] based on their depositional environment (Figure 4). Shales exhibit a range of pore sizes and porosities over multiple length scales (10^{-9} to 10^{-1} meters[9,80,81]) that are created by successive formational processes over geologic time scales.[82] The nanoscale pores can be interparticle, intraparticle, or even inside the organic matter itself,[83] while the natural fractures can be multiple meters long with a millimeter-scale fracture aperture.[47] The intrinsic shale transport properties are dictated by the smaller densely occurring natural microfractures.[84,85] Hydrocarbon gas is stored in these pore spaces as compressed gas and in the kerogen and clay matrix as dissolved gas.[86] Similarly, the polar components of oil facilitate sorption and aid storage in oil-wet nanopores.[87−89] When pressure drawdown is applied to such a system, the compressed oil and gas in the pores is recovered first followed by gas desorbed from the pore walls and diffused from the kerogen and clay matrix[9] resulting in the typical production profile shown in Figure 2.

Clay minerals are predominantly flat 2D structures with shared corners of a silica tetrahedra or alumina octahedra. Of the four major structural groups of clays, kaolinite and Illite are nonswelling in nature[110] while smectite has a tendency to swell.[111−113] Na-smectite, which contains sodium as the dominant exchangeable cation, swells as a result of intercalation of up to four layers of water molecules.[114] Naturally occurring clays are usually an amalgamation of these groups, where Illite is the most common component in unconventional reservoirs. For example, Eagle Ford shale primarily consists of Illite (up to 29% of the total weight of the rock), with little kaolinite;[115] Permian basin shale has an abundance of Illite (∼40% wt.) with sparse volumes of kaolinite and chlorite;[116] Barnett shale has large proportion (∼27% wt.) of Illite with minor smectite;[117] and Marcellus shale has 25% Illite with smaller proportions of chlorite, kaolinite, and smectite.[77]

Generally, shales with high quartz/feldspar and carbonate contents tend to have a higher density of natural fractures:[47]

Table 2. Common Chemical Components in Fracturing Fluid (Figure 1, Pad Step) With Their Main Purpose[123,124] and the Average Volumetric Fracturing Fluid Composition for Fayetteville Shale[a]

product	purpose of chemical	vol. %[121]	example
gelling agent[125]	increase viscosity of the fluid in order to suspend the proppant	0.056%	guar gum[126]
cross-linker[127]	link up different components to retain fluid viscosity at elevated temperatures	0.007%	boric acid[126]
breaker[128]	efficiently remove the polymer gel inside the fracture	0.01%	sodium bromate[126]
proppant[129]	prop open the fractures after fracturing fluid flow-back. Units: ppg = pounds per gallon	0.2 to 0.25 ppg[19]	silica sand[129]
friction reducer[130]	minimize friction of the fluid	0.088%	kerosene[131]
scale inhibitor[132]	prevent scale deposition in the pipes	0.043%	DTPMP[133]
biocide[134]	Eliminate bacteria in the water that produce corrosive byproducts	0.001%	sodium hypochlorite[134]
surfactant[135,136]	Reduce surface tension of the fluid	0.085%	naphthalene[137]
acid	dissolve minerals (like calcite) in the rock and open spaces in the rock matrix	0.123%	HCl
nonemulsifier	prevent formation of emulsions in the fluid	0.085%	lauryl sulfate[137]
clay stabilizer[138]	prevent clay detachment, migration, and swelling	0.06%	KCl[126]
iron control	prevent precipitation of iron	0.004%	ethylene glycol[131]
pH adjustment agent	adjust the ph of the fluid to improve the effectiveness of other components	0.011%	NaOH[137]

[a]Sand and water comprise the remainder of the volume not indicated in the Fayetteville composition of chemical additives.

they are more brittle and therefore generally more amenable to induced fracturing. But some clay- and organic-rich shales, such as the Marcellus and Vaca Muerta,[118] can also contain a high density of natural fractures if catagenesis drives fracture growth.[47] These natural fractures may or may not be open and hydraulically connected. Often they are filled with mineral cements that can range from iron oxide in the Mancos shales[119] to calcite-rich carbonates in the Marcellus shales.[7,47] These infilled fractures can be stronger or weaker than the host rock.[120] The composition of the cement fill is a function of the geochemical environment, reactivity, and physical characteristics of the fracture surface, reservoir temperature, and the size of the fractures.

WATER CHEMISTRY AND SHALE REACTIVITY

Stimulation fluids are engineered to achieve a wide range of properties that aid in fracture generation, fracture longevity, and hydrocarbon production. A broad range of fluid chemistry is introduced across the duration of the hydraulic fracturing operation. These fluids have diverse properties including a low pH to dissolve the matrix and cement in natural fractures, proppants to keep the generated fractures open, a high viscosity to carry the proppant, and breakers designed to manipulate the viscosity of the fluid over various periods of time for easier fluid recovery. These water-based fluids (Table 2)[121,122] need to be stable over a variety of pressure and temperature conditions. Two highly important classes of additives are the gellants, that increase viscosity of the fluid to aid in proppant transport, and friction reducers, that allow injection of high volumes of fluids by reducing the pumping pressures. Besides these, many other types of additives including biocides, anticorrosives, cross-linkers, and oxidative breakers can dramatically affect the structure and geochemical composition of the shale to which they are introduced.

The reactive minerals comprising the shales interact with the stimulation fluid in a variety of ways. Perhaps an obvious outcome is the dissolution of minerals that are prone to solubilization under acidic and oxic conditions (e.g., calcite and pyrite). The pH of the fracturing fluid varies over the course of the injection process due to mixing of fluids during the sequential addition (Figure 1), reaction with the rock, and mixing with formation/pore fluids resulting in steep acidity gradients in the subsurface. Near fracture faces, minerals will initially come into contact with pH < 0 in the form of the acid spearhead followed by significantly larger volumes of neutral to basic (pH ≈ 7 slickwater or pH 9−10 cross-linked gels) solutions. This pH gradient leads to a wide range of coupled dissolution and secondary scaling behavior. Dissolution of cations from the clay layers split and disintegrate the clays. Dissolution time is higher for nonswelling clay (e.g., Illite) compared to swelling clay (e.g., smectite).[139,140] Calcium and magnesium are released from rock during the dissolution of calcite and dolomite minerals.[141] Pyrite is converted to Fe (III) scale by oxidative dissolution and reprecipitation.[142] Barium dissolved from the drilling mud remnants can be reprecipitated as Barite.[56] In some cases, large amounts of strontium-bearing mineral precipitates can form due to the nature of the connate brines.[143] This behavior is complex and often basin specific. For example iron is universally present and iron scale is a persistent problem[107,144] while strontium is of primary concern in the Permian[145] but not in the Marcellus[146] or Eagle Ford plays.

Microbial populations can exert a substantial impact on the chemistry of injected and produced fluids. Though biocides are added in the fracturing fluid to control microbial growth (Table 2), flowback water can still show enhanced microbial activity.[147,148] For example, anaerobic halotolerant bacteria appear to grow[149] potentially as a result of increased subsurface temperature.[134] Sulfate-reducing bacteria[134] generate H_2S gas that sours the oil resulting in sulfide mineral scaling. Furthermore, the gas can be brought on the surface with produced water, where it causes pitting corrosion[148] and is a health hazard. Biofilms, which effectively act as “gels”, can cause formation damage, alter fracture conductivity, and can mobilize and regrow at different spatial locations.[150] Therefore, produced water may require biological treatment prior to reinjection.

Reuse of cleaned produced water inherently involves a higher salinity injectate than freshwater-based fracturing fluid. This requires consideration of the effects of high ionic strength on the formation. Isomorphic substitution in clays (e.g., Al^{3+} by Fe^{3+} in kaolinite[151]) can significantly alter the unit cell parameters without altering the crystalline structure; though it has a critical impact on the adsorption and catalysis processes.[152] Other stimulation fluid−mineral reactions are less intuitive. For example clay minerals have charged surfaces[153] due to the presence of surface exchangeable cations whose chemical nature (effective ionic radius and hydration

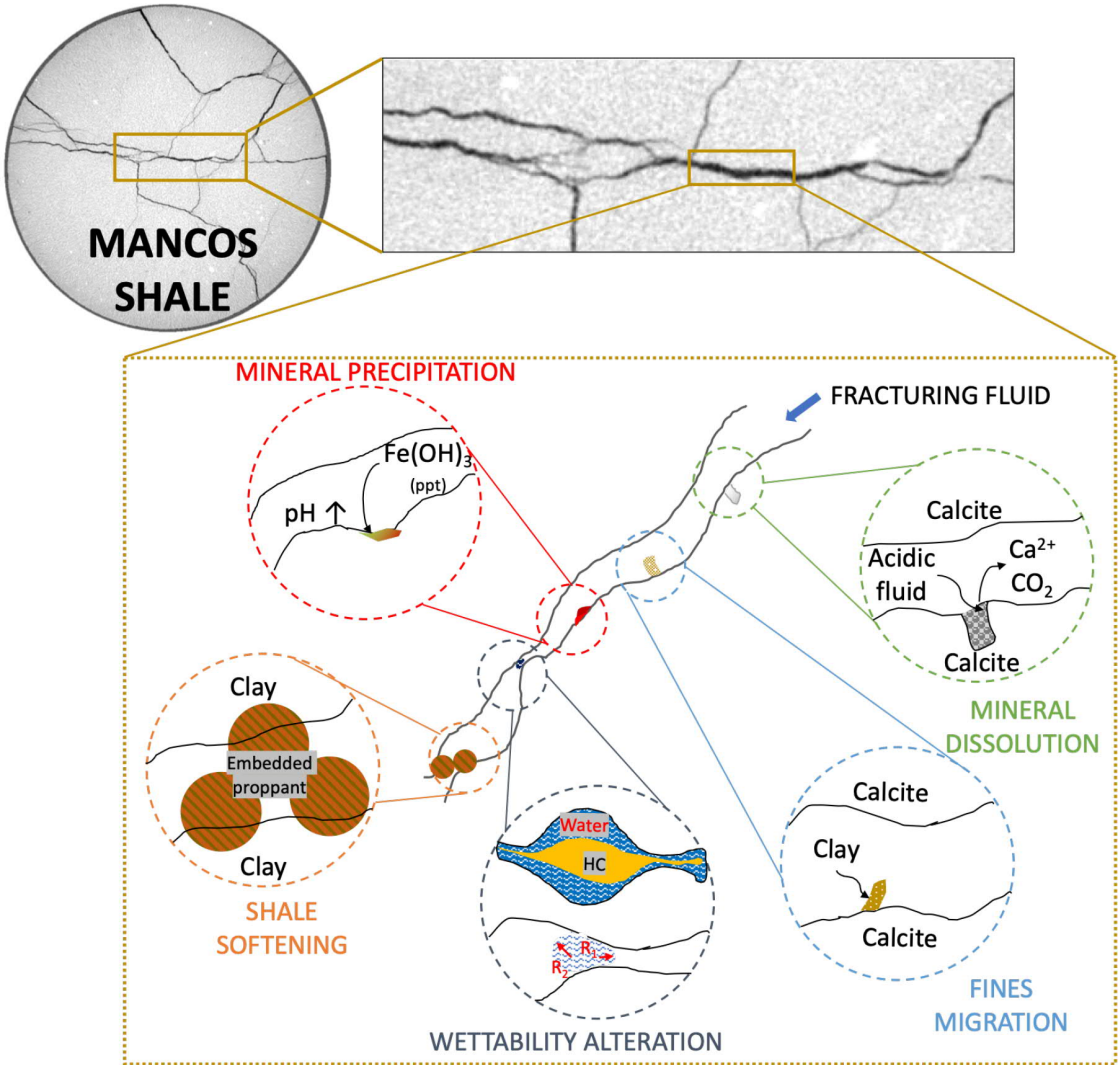

Figure 5. Physicochemical interactions between fracture surfaces and hydraulic fracture fluids can result in decreased or increased fracture conductivity due to shale softening, fines migration, mineral dissolution, mineral precipitation, and wettability alteration. Injection of the highly acidic spearhead causes mineral dissolution (primarily carbonates), resulting in minerals, like K-feldspar, being exposed and ultimately being released as "fines" in the flow pathway. The dissolution also causes the pH conditions to change, ions released from initial dissolution become supersaturated and can precipitate in different spatial locations such as fracture surface and shale matrix. Furthermore, the acid etches the fracture surface and reduces the surface hardness of the shale, which enables proppants to be embedded in the surface ultimately reducing the flow area. Wettability is altered by chemical interactions between the surfactants and the matrix, resulting in a change in the capillary pressures. This can potentially trap the water phase in the micropores by creating a water block. Original micro-CT scan available at Luo et al.[119]

energy[154]) govern the physicochemical properties of the clay, and consequently interactions with the stimulation fluid. These exchangeable cations obtain complete or partial hydration shells based on their enthalpies of hydration which make the clay mineral hydrophilic in nature.[154] The layer expands in the first step with some water adsorption and then the second step increases the water uptake without swelling.[155] The attached water molecules also tend to have different physicochemical properties than the bulk water.[156] This creates three fundamental classes of interaction between the water molecules in the stimulation fluid and the clay minerals:

1. Swelling, This phenomenon occurs when the clay mineral expands after interacting with water.[112,157] The two prominent mechanisms of clay swelling:
    - Osmotic swelling, This occurs when there is a difference in the concentration of cations in the interlayer space of shale and in the bulk solution. Water is drawn from the less concentrated water-based stimulation fluid to the shale interlayer region with a higher cationic concentration.[158,159] This mechanism is ion-dependent: Na^+-saturated smectite show a large volume change compared to K^+-saturated smectite,[160] which preferentially form crystalline hydrates. Overall, the use of produced waters with high Na^+ will result in enhanced swelling, while a high background K^+ or addition of KCl to reinjected water may aid in inhibiting swelling.
    - Crystalline swelling, This stepwise process is caused by the hydration of the exchangeable cations of the clay (with lower water content) resulting in adsorption of multiple discrete layers

of water on the clay surfaces.[114,160] Negatively charged clay layers are held together by the interlayer cations that hydrate upon interaction with the polar water molecules, rearranging such that spacing is increased between the clay layers.[113,161] This interlayer spacing is dependent on the thermodynamic potential that is constrained by the pH, temperature, and pressure.[160]

2. Dispersion, Dispersion is a rapid process in which individual layers of the clay mineral are separated and dispersed in solution with no interactions between the layers.[114,162] Hydration of clay minerals causes the pore pressure to be greater than the strength of the bond between the clay minerals[163] and results in exfoliation of clay blocks into colloidal-size fines.[164] The surface charge, pH, and clay composition are factors that control clay dispersion.[165−167] Dispersed smectite clays have variable shapes,[167] for example, the swelling clay Na^+-montmorillonite disperses into individual sheet-like layers[168] while the nonswelling kaolinite readily disperses in the presence of water or noninhibiting drilling mud[164,169] to form a colloidal suspension.[164,170] Studies[171−173] have shown that bacterial action can change the surface area, cation exchange capacity, and the layer charge on clays which can impact dispersion.
3. Flocculation or aggregation, The addition of polymer macromolecules can destabilize the colloidal dispersion and cause the particles to aggregate and come out of suspension either by bridging the particles (attaching to the surface of two individual particles) or by neutralizing the surface charge on the particle.[174] Flocculation is also dependent on ionic strength; higher ionic strength results in lower Debye length and thinner electric double layer which leads to charged patch attraction[175] and ultimately structural alteration.[176] The particles "feel each other" leading to aggregation.[162,177]

Clay-stabilizers (Table 2) are generally added to mitigate these clay detachment, migration, and swelling processes in shales. But adding high molecular weight stabilizers can result in pore-blocking[178] that causes water-locking damage. Furthermore, prolonged exposure to KCl showed increased brittleness in the shale.[179]

EVOLUTION OF SHALE FLOW CHANNELS DUE TO REACTIVE TRANSPORT

During the hydraulic fracturing process large volumes of fracturing fluid (median ~6000 m^3 (6 million L)[124]) are injected in a given well. A significant proportion (60−90%[19,180]) of this fluid is never recovered during subsequent production though the total fluid produced can exceed the total injected volume. The large hydraulic pressure difference between the shale matrix and the fracture primarily results in fluid seepage inside the matrix[181] and the recovered fluid is mostly formation water.[182] Furthermore, spontaneous imbibition due to capillary pressure[183−185] and the large osmotic potential due to the high-salinity contrast between the fracturing fluid and connate water[122] also contributes to substantial loss of injected fluid in the reservoir.

Fluid and solid physio(geo)chemical interactions on the shale surface can result in increased or decreased fracture conductivity.[186,187] These changes in fracture conductivity are controlled by multiple parameters, including but not limited to, closure stress, rock mechanical properties, surface mineralogy, proppant type, fluid flow rate, fracture surface topography, and wettability of the pathways.[73,188] These parameters usually act simultaneously and result in complex evolution of the fluid conductive pathway(s) over time. Here we discuss five major mechanisms (shale softening, mineral dissolution, mineral precipitation, fines migration, and wettability alteration) that can influence the flow potential of the shale over the course of stimulation and production (Figure 5).

Shale Softening. Clay minerals in shales are reactive with water.[186] Injection of water-based fluids, as opposed to oil-based fluids, into shales causes a multitude of (problematic) effects including clay swelling (increase in volume) and ultimately shale softening.[189,190] Shale softening is the phenomenon where the mechanical properties of the shale such as elasticity, hardness, and strength deteriorate.[191] This can result in embedment of proppant, more difficult fracturing, and creep deformation in shales[189] that effectively reduces the formation conductivity.

Smectite shales are particularly known for the difficulties associated with clay swelling during the drilling phase. Water-based drilling muds have been largely phased out of drilling in shales due to the long-term interaction between water and clay causing constricted boreholes by clay swelling and associated mechanical instability due to the altered stress state of the shale.[158,192] An oil-based drilling mud or an inhibitive water-based drilling mud is used instead to overcome such issues. The additives to the mud (e.g., KCl) inhibit the hydration of the clays and prevent the clay from absorbing water and swelling and/or dispersing.[193−195] As return water is increasingly reused, this high-salinity solution is expected to behave similarly, i.e. inhibit clay swelling and dispersion by blocking the hydration of clays in the shale matrix. Recent experiments[46] show that the injection of high-salinity brine recovers permeability of the rock by reattaching the dispersed clay fines.

All clays are not swelling in nature (Section Water Chemistry and Shale Reactivity), yet interestingly the shale softening phenomenon is observed in shales with all types of clay. Illite and kaolinite are nonswelling clays; the thickness of their electrical double layer is on the order of or even thicker than the mean pore sizes in shales.[167] The clays on the shale outer surface on the opposite ends of these micropores therefore can have an overlap in the electrical double layer, resulting in an increased electrostatic repulsion in the charged external clay surface that leads to increased hydration pressure.[116,189] Clay content, specifically of the nonswelling clays,[169] is the primary cause of the difference between the fracture conductivity loss for a variety of shale samples:[196] Barnett shale (55% clay) showed an 80% loss of the original fracture conductivity (15 mD-ft to 0.41 mD-ft) after water injection compared to a 20% loss (242 mD-ft to 191 mD-ft) in the Eagle Ford shale (12% clay) and a 6% loss in a Berea sandstone sample.

Tuscaloosa Marine Shale (TMS) is a clay-rich (~48% clay content) play located in the U.S. Gulf Coast with a potential of 7 billion barrels of recoverable oil.[197,198] The TMS contains a high proportion of swelling clays (12% smectite and 14% Illite) and nanoindentation tests suggest it is a soft ductile rock[199] making the hydraulic fracturing operations difficult. The soft shale allows the proppant to be embedded on the fracture surface resulting in partial closure of the fracture, leading to significant reduction in the fracture conductivity and ultimately

the hydrocarbon production.[200−202] Furthermore, the softness of the rock makes it prone to disaggregation if the drawdown is high when putting the well back on production.

Mineral Dissolution. As mentioned earlier (Section Water Chemistry and Shale Reactivity), mineral dissolution is purposefully induced by the acid spearhead (Figure 1, Step 1) to initiate fracturing. Because calcite and gypsum are more soluble at low pH, carbonate-rich shales are prone to quicker dissolution and can create surface structures such as channels, cavities, and/or rings depending on the mineral distribution.[54] This dissolution potentially increases the porosity of the shale but does not necessarily increase the permeability as expected.[203] Noiriel et al.[204] proposed that the calcite and clay minerals dissolve simultaneously in an argillaceous limestone, but a microporous clay coating forms on the dissolution sites resulting in narrowed pathways and a subsequent decline in dissolution rate. In contrast, Wu and Sharma[54] found that these surface changes can form asperities due to nonuniform dissolution that can improve fracture conductivity. The combined effect of dissolution can therefore either be net gain or net loss of conductivity, and the relationship is largely specific to the lithology of the basin and microenvironments therein.

Dissolution of calcite, dolomite, and other carbonate minerals generates dissolved carbonate ions that are capable of neutralizing the acid spearhead. The buffering capacity of the shale largely depends on the total amount and accessibility of carbonate minerals and thus not only varies between shale plays but also within a shale play as different localities are stimulated. Li et al.[109] exposed different shale formations to synthetic fracture fluid and found that carbonate dissolution extended deeper into matrices with less neutralizing capability compared to carbonate-rich shales that can more readily neutralize the acid front (100−200 μm into the matrix for the carbonate-poor Marcellus shale vs 30−40 μm for the carbonate-rich Eagle Ford shale).

The specific type of carbonate mineral can also have an impact on dissolution. Jew et al.[205] exposed Green River ground shale (23 wt % calcite and 29 wt % dolomite) to synthetic hydraulic fracturing fluid and observed preferential dissolution of calcite over dolomite. Similar widespread dissolution of calcite and minimal dissolution of dolomite have been previously observed in Marcellus shale[206] that is attributed to the differences in relative solubilities and kinetics of dissolution between calcite and dolomite.[207,208]

A second widespread class of dissolution pathways created during fracturing of shale reservoirs are associated with the highly oxidative state of the injection fluid. Extensive studies have demonstrated oxidative dissolution of Fe(II)-bearing phases (e.g., pyrite and Fe(II) bound directly to organic matter) in shales.[106,107,141,142] In particular, the oxidative dissolution of pyrite can alter pore structure,[206,209] mobilize heavy metals,[131] and release iron and sulfate ions that lead to secondary mineral precipitation[109] (discussed later in Section Mineral Precipitation). At low pH, oxidation of Fe(II) to Fe(III) is relatively slow; however, Jew et al.[107] found that bitumen solubilized from the shale by the organics in fracture fluid formulation reduces the inhibiting effect of the acid spearhead on Fe(II) oxidation and enhances oxidation at low pH. The mechanism by which bitumen influences Fe(II) oxidation remains unknown.

The presence of other competitive ions, such as those present in high-salinity produced water, can have a detrimental effect on mineral solubility. In the absence of a common ion and in low ionic strength, the solubility of a mineral increases as the ionic strength increases. However, at high ionic strengths (such as those observed in produced water), the ability for water to solvate ions becomes limited; the counterion effect can also be significant. Ali and Hascakir[103] exposed crushed samples of Eagle Ford and Barnett shales to deionized water. The former has a higher proportion of gypsum compared to the latter but the results showed that the sulfate concentration in the two shales was similar. Based on Le Chatelier's principle they concluded that the presence of large concentrations of the aqueous calcium ions (released from the dissolved calcite in the calcite-rich Eagle Ford) causes a decline in solubility resulting in a lower amount of gypsum being dissolved. Thus, the presence of high carbonate levels not only increases scaling potential (Section Mineral Precipitation) but also makes the stimulation fluid pH more difficult to control.[210]

Mineral Precipitation. In general, the scale formation process involves four phases:[211] solution supersaturation, nucleation, crystal growth, and agglomeration. Thermodynamically, precipitation becomes feasible when the activity of ions in solution exceeds the saturation threshold with respect to a given mineral. The scaling ions subsequently form microaggregates on the shale surface that become nucleation centers for crystallization. These crystals then continue to grow into a scale film on a surface and eventually into a scale deposit via the sorption of additional scaling ions from solution. Many factors lead to scale deposition including incompatible water, pH value, pressurization, salt content, and temperature.[212] The potential for secondary mineral precipitates to irreversibly clog porosity to reduce hydrocarbon production from the shale matrix, damage well productivity, and reduce overall extraction efficiency is a well-recognized concern, particularly when reusing high-salinity produced water[47,101,213,214] (Figure 6).

Solution pH plays a critical role in the formation of secondary mineral precipitates.[107] Multivalent cations, especially Ca^{2+}, Fe^{3+}, and Ba^{2+}, are generated from the acid spearhead via dissolution of minerals. If not properly mitigated, these cations can precipitate due to the increased pH caused by a combination of carbonate dissolution and mixing with formation water.

Calcium (released via the dissolution of calcite, dolomite, anhydrite, and other calcium-bearing minerals) frequently combines with sulfate generated from anhydrite dissolution,[215] additives (including the use of persulfate breakers),[45,209] and oxidative dissolution of pyrite[109,142] to form gypsum. The relative importance of these different factors is likely dependent on the shale play. Osselin et al.[215] performed $\delta^{34}S$ and $\delta^{18}O$ isotopic analysis of flowback water from the Montney Formation (Canada) and found that the excess sulfate in the collected samples was mainly derived from anhydrite dissolution, and not from persulfate breaker or pyrite oxidation. However, Harrison et al.[142] concluded that oxidation of pyrite was the primary source of the sulfate in solution in their experiments using Eagle Ford samples.

Ferrous iron (Fe(II)) in the shale dissolved from various mineral phases including pyrite, siderite, and chlorite can oxidize and subsequently precipitate as Fe(III)-(oxy)-hydroxides.[59] For example, Flynn et al.[216] observed Fe(III) oxyhydroxides that were silica-enriched in produced water from the Duvernay Formation in Alberta, Canada. Jew et al.[107] observed that in systems with low pH buffering capacity (i.e.,

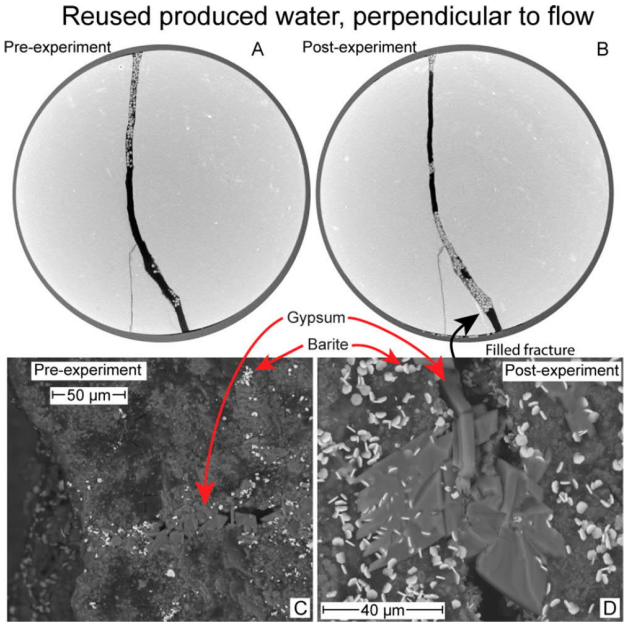

Figure 6. X-ray CT of shale before (A) and after (B) exposure to recycled hydraulic fracturing fluid. Note the secondary mineral precipitation inside the small fracture in (B). (C,D) SEM images of fracture in (B), partially filled with Barite and gypsum. Reproduced from Paukert Vankeuren et al.[45]

low carbonate content), dissolved Fe(II) remains in solution for a significant amount of time, allowing transport to occur prior to oxidation and precipitation of Fe(III)-bearing solids. Conversely, systems with high pH buffering capacity (i.e., high-carbonate content) result in Fe(III)-bearing phases precipitating near pyrite framboids, indicating that the released iron did not travel far once dissolved. Therefore, reusing produced waters high in Ca^{2+}, like in Bakken shale,[217] can cause early near-wellbore deposition of iron precipitate.

Barite ($BaSO_4$) is another commonly observed form of scaling in hydraulic fracturing systems, particularly in the Marcellus shale. The main source of the barium is still under debate, with opinions ranging from release from minerals due to weathering under high ionic strength conditions[218] to dissolution and reprecipitation of barium from drilling mud[56] to brines adjacent to and/or below the Marcellus shale.[219] As more fluid is injected during the hydraulic fracturing process, more connected fractures are created. A recent study[220] showed rapid Ba^{2+} precipitation at the freshly generated fracture surface, which has a high reactive surface area. Furthermore, the variation of the fracture aperture in the connected network is expected to affect the precipitation dynamics: larger aperture fractures have a lower flow rate at the fracture surface, which results in a higher saturation and ultimately a higher chance of mineral precipitation. This chance is enhanced when using produced water with a higher dissolved cation concentration.[221]

Other divalent ions can readily form secondary mineral precipitates in flowback water. Strontium, which is found naturally in the shales itself or in the formation water of some plays, readily precipitates as celestite ($SrSO_4$) or strontianite ($SrCO_3$).[215] In the presence of high concentrations of barium, Barite and celestite can coprecipitate as a solid solution in the flowback fluid; this is likely associated with the cooling of produced water at surface temperatures and the subsequent creation of supersaturated conditions that drive precipitation.[216]

Numerous studies have demonstrated the effectiveness of various scale inhibitors in preventing precipitation in conventional oil and gas production. Generally, there are three types of scale inhibitors: chelation agents, phosphate/phosphonate-based inhibitors that can prevent crystal growth, and polymeric inhibitors that inhibit nucleation.[212] These are targeted to common scalants such as calcium carbonate,[222] calcium sulfate,[223,224] barium sulfate,[119,133,223,225−227] strontium sulfate,[223,226] and iron-based[228,229] minerals. However, the ability of scale inhibitors to prevent these precipitation reactions in unconventional systems is unclear. Importantly, brine chemistry can dramatically influence the effectiveness of scale inhibitors.[230] Certain scale inhibitors, such as diethylenetriamine penta(methylene phosphonic acid) (DTPMP), have been found to precipitate with calcium in the carbonate-rich Eagle Ford shale[231] and with Fe- and Al-bearing minerals on biotite.[232] Additionally, the ability of DTPMP[233] and other traditional scale inhibitors such as ethylene glycol[234] to prevent Barite precipitation under highly saline conditions is limited. Reusing high-salinity produced water (already prone to mineral precipitation[45,180]) laced with these inhibitors therefore increases mineral precipitation and results in further constriction of the fluid flow pathways.

Fines Migration. Particle retention caused by fines migration has been studied extensively[235−237] in different domains of science and is well understood in uniform media.[238] The two main mechanisms studied are particle straining and surface deposition. The former is prominent for larger-sized particles (micrometer-scale) and works via the process of size exclusion where particles larger than the pore throat are trapped at the pore entrance.[239] The latter is prominent for the lighter, smaller-sized particles (submicron colloidal scale) that are more prone to surface attachment due to the electrostatic and van der Waals surface forces.[240] Both of these mechanisms result in reduction of the flow area that leads to increased probability of particle retention.[241] Particle entrapment in nonhomogeneous media, like vuggy carbonates, has been recently studied and the pore-size anisotropy is found to affect significantly the particle entrapment characteristics of the permeable medium.[242,243]

Fines can be generated in shales due to multiple factors, including but not limited to matrix dissolution, clay dispersion, fracture surface spalling, and proppant failure.[186,196] This particulate movement is highly dependent on the shale surface minerals[204,244] and the fluids interacting with them, and can be caused by a combination of chemical and physical interactions. The generated fines, like the reactive clays, can flocculate[245] in high-salinity environments[246] (with higher ionic strength) to create larger-sized particles that potentially cause more permeability loss in the narrow fracture pathways. This effect is likely to be exacerbated by reuse of produced water which is inherently more saline than freshwater injections.[247] The high-salinity of the base fluid also limits the amount of proppant[248] that can be carried by the fluid, which results in narrower fractures and therefore has the potential for a more pronounced permeability decline due to clogging by the larger-sized particles.

Natural microfractures in low-permeability shales dictate intrinsic transport properties[84,85] and become connected during hydraulic fracturing to form the major pathways for hydrocarbon production.[249,250] Fines generated in one part of

the rock are mobilized by the fluid and can reach distant locations via these microfractures with smaller fracture apertures. The fines can potentially plug up narrow conductive pathways[204,251−253] by size exclusion and/or surface deposition, and drastically reduce the flow potential of the rock system.[254] The generation of fines can potentially expose a different mineral surface on the fracture wall, with a unique wettability. This can change the wetting nature of the reservoir rock[255] and result in further reduction in conductivity.

Matrix Dissolution. Highly reactive (e.g., calcite-rich) rock fabric dissolves in the presence of the acidic fracturing fluid and dislodges any associated relatively inert grains such as quartz, clays, and organic matter,[54,256] which act as fines. Recent studies[203,252,257] have found that fines are commonly created by matrix dissolution induced chipping, where part of the carbonate matrix is dissolved and releases the undissolved part as a coherent grain. Furthermore, prolonged interaction with the fracture fluid during the "soaking" period (extended shut-in before production intended to enhance fracture characteristics and ultimately increase production) can result in the dissolution of iron and manganese oxides.[45] Reservoir case studies[258] have shown sudden drops in wellhead pressure after extended times (>1000 days), which have been associated with fines generation. As mentioned earlier (Section Mineral Precipitation), reusing high-salinity produced water increases the chances of mineral precipitation on the shale surface, that can be mobilized as fines if the reactive rock underneath is dissolved by the acidic nature of the fracturing fluid.

Proppant Failure. Low-strength, low-concentration proppants interacting with rough fracture surface experience extreme stress conditions that can result in grain crushing.[259] Loose packing of proppants consistently resulted in more proppant crushing than dense packing.[50] Reusing high-salinity produced water alters the rheological character of the fracturing fluid and reduces its proppant carrying capacity;[248,260] this in turn reduces the proppant packing efficiency which results in a looser pack that is more prone to grain crushing. The crushing creates a mixture of particles: some which are too large to pass through the pore throats and some which are small enough to reach further into the pore network.[261] Grains of intermediate size act as fines and migrate with the formation fluid causing permeability reduction at a range of different locations inside the formation.[262,263]

Fracture Surface Spalling and Matrix Crushing. Hydraulic fracturing uses large volumes of high pressure fluid to break open the rock along planes of tensile weakness, creating rough surfaces.[264,265] As the fluid is dissipated, the pressure inside the rock decreases and the normal stress forces the fractures to close.[256] Due to the roughness of the fracture surfaces, the closure is not inherently a perfect seal and, in localized regions, the injected fluid velocity may be high enough to "spall" the fracture surface and create debris that act as fines.[266] Furthermore, the high pressures applied during hydraulic fracturing also crushes/breaks the rock which produces particle fines. Proppants embedding into the fracture surface due to shale softening can generate such fines as well.[189]

Clay Dispersion. Clay dispersion mechanisms are discussed in detail in Water Chemistry and Shale Reactivity Section. The swelled clay platelets are pulled apart and disintegrated,[169] and nonswelling clays such as Illite and kaolinite are mobilized with the fluid, creating the potential to block flow pathways by the process of surface deposition. Reusing high-salinity produced water,[247] specifically with high K^+ content, can cause these colloidal-sized clay fragments to flocculate[267] and gel to prevent gravity settlement,[245,268] resulting in increased formation damage by particle straining.

Wettability Alteration. Shale wettability is reported to vary from water-wet to mixed-wet to oil-wet (Figure 7)[51,269−271] based on the pore connectivity,[272] matrix

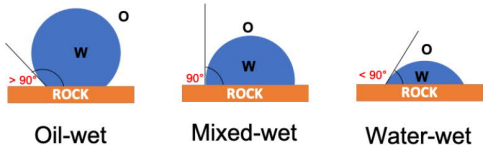

Figure 7. Three types of wettability found in rocks: oil-wet, mixed-wet, and water-wet.

composition, and fluid composition[271] of the shale. The wettability of the rock governs how the fluids interact with the fracture faces. For example water-wet rocks are coated with a water-film that separates the hydrocarbon from the rock surface such that the hydrocarbon exists as a disconnected ganglia within the pores.

Large amounts of water, with dissolved additives such as surfactants,[273] may remain inside the formation for as little as a few days before flowing back or could be retained permanently (no recovery) and are typically held within the fracture face over a length scale of a few inches.[21] The component of the shale porosity present in the organic matter is assumed to be oil-wet, while interdetrital porosity tends to be more water-wet. The lost fluid has the tendency to change the surface wettability of the shale pores from oil-wet to water-wet.[131,136,274] The water phase in the micropores can become trapped due to the change in capillary pressures[275,276] or as a result of forming a connected hydrocarbon-phase ganglia[50] that leaves the water-phase trapped near the water-wet pore surface (Figure 5); this ultimately reduces the hydrocarbon recovery.[277,278] Multiple processes including heat[271] and surfactant treatment[184] have been proposed to mitigate this damage and enhance hydrocarbon recovery.

Wettability alteration is impacted by a variety of factors: ionic concentration,[279] presence of divalent cations,[51,279] pH, pressure,[280] and temperature.[255,281] Of these, the most prominent are the concentrations of divalent ions that make the system oil-wet[279] by adsorbing these ions and reducing the surface potential, thus increasing the contact angle. Injecting recycled water, with larger concentrations of divalent ions such as Ca^{2+},[217] may make the system more oil-wet[279] and therefore less prone to these water blocks in the smaller pores and fractures.

SUMMARY

The physicochemical interactions of fracturing fluid with shales are complex, with multiple processes occurring simultaneously at different length scales. The fracturing fluid interacts with the rock matrix and formation fluid, and can result in evolution of the newly generated fluid flow pathways. Using produced fluid (with high-salinity and TDS) can complicate this behavior further due to shifts in the fracturing fluid composition and its properties.

High concentrations of multivalent cations negate the effect of cross-linkers and cause stability issues, while high Na^+ content combats the viscosifiers to reduce viscosity and increase proppant settling velocity, and oxygen mixing

promotes growth of aerobic bacteria and aids in oxidation of Fe(II) to Fe(III). Reactive clay minerals interact with fresh water fracturing fluid and soften up, resulting in increased embedment of the proppant and therefore reduced conductivity. A higher salinity base fluid will have multiple contrasting impacts: the high-salinity will inhibit clay dispersion and improve conductivity by reattaching the dislodged fines. At the same time, high-salinity fluid will require significantly higher amounts of gellant and cross-linkers to attain the same viscosity as freshwater fluid. Generally they will have a lower viscosity and carry less proppant, resulting in smaller apertures and less stable fractures.

Minerals, such as carbonates, rapidly dissolve in the low-pH fresh water fracturing fluid creating void space and improving conductivity. Cleaned high-salinity base fluids will have a higher concentration of dissolved ions which will reduce the rate of dissolution of these minerals from the shale surface. Alternatively, the dissolution of one mineral can cause another mineral to precipitate from solution and deposit in the flow path, reducing conductivity. For example, the change from pyrite to ferrihydrite results in a nearly 30% volume increase on a per mole basis. A high-salinity base fluid, specifically containing elevated concentrations of alkali earth metals, will cause mineral precipitation and scale formation in the near wellbore region, resulting in reduced flow pathways near the injection site and subsequently a higher chance of fracture screen out.

Mineral fines are generated by multiple processes (spalling, dissolution, proppant failure, or clay dispersion) in one part of the rock and deposited in a different spatial location, potentially causing detrimental effects on conductivity. A high-salinity base fluid will exacerbate fines generation by more proppant crushing and ultimately fracture spalling due to looser proppant packing and fines deposition.

It has been shown that fresh water fracturing fluid can alter the wettability of the rock as a result of both ionic concentration and low pH. This changes the relative permeability of the flow pathways reducing the hydrocarbon production of the rock. A high-salinity base fluid may amplify this problem with the abundance of divalent ions in solution.

From this basis, the expanded application of reused produced water requires further research in several key areas. Present produced water cleaning practices emphasize the removal of oil/grease phase and suspended solids using membranes and settling tanks. Based on this review and synthesis, additional remediation steps would be necessary to remove microbes, organics, and monovalent and divalent ions which can cause a plethora of detrimental effects upon interaction with the shale formation. Thus, a grand challenge is the need to achieve effective, economical, and rapid cleaning strategies for these large quantities of water. Permian basin, for example, produces 15 times more water than Marcellus where water reuse is being currently practiced. Many techniques such as nanofiltration, forward osmosis, and mechanical vapor compression are available, but they lack in many of the aforementioned criteria. Furthermore, this review highlights several areas where there is simply insufficient information available to make an educated assessment. For example, there is sparingly little literature reporting the composition of organics present in produced water, or how these organics may further interact with the reservoir if they are reintroduced. It is evident that organics can bind with a variety of minerals commonly present in shales and may alter the wettability of the fracture surfaces and matrix interior. Ultimately, the key metric of success in the efficacy of cleaning and reusing these produced waters will manifest in the long term (months to years) production rates of wells stimulated in this manner. For this multiple pilot tests are needed across a variety of shale plays.

Currently, hydrocarbon production exponentially declines over time in unconventional wells (Figure 1). In order to improve hydrocarbon recovery new mitigation strategies for reducing shale softening, controlling secondary mineral precipitation, and resolving water blocks are needed. Furthermore, to maximize the reuse of produced water, fracturing fluid mixtures that can tolerate high-salinity waters need to be developed. For this, focus has to include characterization of the produced fluid as well as the shale reservoir. Coupling between fluid-shale reactivity, advective transport through fractures, and imbibition into the shale matrix needs to be made within forward and predictive modeling frameworks. Each of these components are necessary to describe the multiscale fabric of shale flow paths and thus translate between pore- and reservoir-scales.

AUTHOR INFORMATION

Corresponding Authors

Hasan Javed Khan − *Department of Geology, University of Illinois at Urbana−Champaign, Urbana, Illinois 61801, United States;* orcid.org/0000-0001-8867-8438; Email: hasanjk@illinois.edu

Jennifer L. Druhan − *Department of Geology, University of Illinois at Urbana−Champaign, Urbana, Illinois 61801, United States;* orcid.org/0000-0003-0200-3988; Email: jdruhan@illinois.edu

Authors

Eleanor Spielman-Sun − *Stanford Synchrotron Radiation Lightsource, SLAC National Accelerator Laboratory, Menlo Park, California 94025, United States;* orcid.org/0000-0001-9626-2969

Adam D. Jew − *Stanford Synchrotron Radiation Lightsource, SLAC National Accelerator Laboratory, Menlo Park, California 94025, United States;* orcid.org/0000-0002-6167-8769

John Bargar − *Stanford Synchrotron Radiation Lightsource, SLAC National Accelerator Laboratory, Menlo Park, California 94025, United States;* orcid.org/0000-0001-9303-4901

Anthony Kovscek − *Department of Energy Resource Engineering, Stanford University, Stanford, California 94305, United States;* orcid.org/0000-0003-1336-384X

Notes

The authors declare no competing financial interest.

ACKNOWLEDGMENTS

This work was supported as part of the Center for Mechanistic Control of Water-Hydrocarbon-Rock Interactions in Unconventional and Tight Oil Formations (CMC-UF), an Energy Frontier Research Center funded by the U.S. Department of Energy, Office of Science under DOE (BES) Award DESC0019165.

REFERENCES

(1) U.S. Energy Information Administration.*International Energy Outlook 2019*. 2019, 85.

(2) U.S. Energy Information Administration. *Annual Energy Outlook 2019 with projections to 2050*; 2019; p 83.

(3) Yaalon, D. Mineral composition of the average shale. *Clay Miner.* **1962**, *5*, 31−36.

(4) Schultz, L. G.; Tourtelot, H.; Gill, J.; Boerngen, J. *Composition and properties of the Pierre Shale and equivalent rocks, northern Great Plains region*; USGS, 1980.

(5) Javadpour, F.; Moravvej Farshi, M.; Amrein, M. Atomic-Force Microscopy: ANew Tool for Gas-Shale Characterization. *Journal of Canadian Petroleum Technology* **2012**, *51*, 236−243.

(6) Vega, B.; Andrews, J. C.; Liu, Y.; Gelb, J.; Kovscek, A. Nanoscale visualization of gas shale pore and textural features; *Unconventional resources technology conference* 2013; pp 1603−1613.

(7) Vega, B.; Ross, C. M.; Kovscek, A. R. Imaging-Based Characterization of Calcite-Filled Fractures and Porosity in Shales. *SPE Journal* **2015**, *20*, 810−823.

(8) Wood, D. A.; Hazra, B. Characterization of organic-rich shales for petroleum exploration & exploitation: A review-Part 1: Bulk properties, multi-scale geometry and gas adsorption. *J. Earth Sci.* **2017**, *28*, 739−757.

(9) Javadpour, F.; Fisher, D.; Unsworth, M. Nanoscale Gas Flow in Shale Gas Sediments. *J. Can. Pet. Technol.* **2007**, *46*. DOI: 10.2118/07-10-06

(10) Salama, A.; Amin, M. F. E.; Kumar, K.; Sun, S. Flow and Transport in Tight and Shale Formations: A Review. *Geofluids* **2017**, *2017*, e4251209.

(11) Bitumen and heavy crudes: the energy security problem solved? *Oil and Energy Trends*, 2006, *31*, 3−6, _eprint: https://onlinelibrary.wiley.com/doi/pdf/10.1111/j.1744-7992.2006.310603.x.

(12) Makogon, Y. F.; Holditch, S. A.; Makogon, T. Y. Natural gas-hydrates — A potential energy source for the 21st Century. *J. Pet. Sci. Eng.* **2007**, *56*, 14−31.

(13) Gadonneix, P.; de Castro, F. B.; de Medeiros, N. F.; Drouin, R.; Jain, C.; Kim, Y. D.; Ferioli, J.; Nadeau, M.-J.; Sambo, A.; Teyssen, J. et al. *2010 Survey of Energy Resources*; Citeseer2010; p 593.

(14) *Assumptions to the Annual Energy Outlook 2020: Oil and Gas Supply Module*; US EIA, 2020; p 22

(15) Clark, C. E.; Han, J.; Burnham, A.; Dunn, J. B.; Wang, M. *Life-cycle analysis of shale gas and natural gas*; Argonne National Laboratory, 2012.

(16) Clark, C. E.; Horner, R. M.; Harto, C. B. Life Cycle Water Consumption for Shale Gas and Conventional Natural Gas. *Environ. Sci. Technol.* **2013**, *47*, 11829−11836.

(17) Vengosh, A.; Jackson, R. B.; Warner, N.; Darrah, T. H.; Kondash, A. A Critical Review of the Risks to Water Resources from Unconventional Shale Gas Development and Hydraulic Fracturing in the United States. *Environ. Sci. Technol.* **2014**, *48*, 8334−8348.

(18) Zhang, D.; Yang, T. Environmental impacts of hydraulic fracturing in shale gas development in the United States. *Petroleum Exploration and Development* **2015**, *42*, 876−883.

(19) King, G. E. Thirty Years of Gas Shale Fracturing: What Have We Learned?; *SPE Annual Technical Conference and Exhibition*, 19-22 September, Florence, Italy,2010.

(20) Li, Q.; Xing, H.; Liu, J.; Liu, X. A review on hydraulic fracturing of unconventional reservoir. *Petroleum* **2015**, *1*, 8−15.

(21) Byrnes, A. P. Role of induced and natural imbibition in frac fluid transport and fate in gas shalesfor the Hydraulic Fracturing Study: Fate and Transport. In *Technical Workshops for Hydraulic Fracturing Study*; Chesapeake Energy Corporation, 2011; Vol. *70*.

(22) Scanlon, B. R.; Reedy, R. C.; Male, F.; Walsh, M. Issues Related to Transitioning from Conventional to Unconventional Oil Production in the Permian Basin. *Environ. Sci. Technol.* **2017**, *51*, 10903−10912.

(23) Kondash, A. J.; Lauer, N. E.; Vengosh, A. The intensification of the water footprint of hydraulic fracturing. *Science Advances* **2018**, *4*, eaar5982.

(24) Estrada, J. M.; Bhamidimarri, R. A review of the issues and treatment options for wastewater from shale gas extraction by hydraulic fracturing. *Fuel* **2016**, *182*, 292−303.

(25) Scanlon, B. R.; Ikonnikova, S.; Yang, Q.; Reedy, R. C. Will Water Issues Constrain Oil and Gas Production in the United States? *Environ. Sci. Technol.* **2020**, *54*, 3510−3519.

(26) Shaffer, D. L.; Arias Chavez, L. H.; Ben-Sasson, M.; Romero-Vargas Castrillón, S.; Yip, N. Y.; Elimelech, M. Desalination and Reuse of High-Salinity Shale Gas Produced Water: Drivers, Technologies, and Future Directions. *Environ. Sci. Technol.* **2013**, *47*, 9569−9583.

(27) McCurdy, R. *Underground injection wells for produced water disposal*. Proceedings of the Technical Workshops for the Hydraulic Fracturing Study: Water Resources Management. EPA. 2011.

(28) Keranen, K. M.; Weingarten, M.; Abers, G. A.; Bekins, B. A.; Ge, S. Sharp increase in central Oklahoma seismicity since 2008 induced by massive wastewater injection. *Science* **2008**, *345*, 448−451.

(29) Frohlich, C.; DeShon, H.; Stump, B.; Hayward, C.; Hornbach, M.; Walter, J. I. A Historical Review of Induced Earthquakes in Texas. *Seismological Research Letters* **2016**, *87*, 1022−1038.

(30) Lutz, B. D.; Lewis, A. N.; Doyle, M. W. Generation, transport, and disposal of wastewater associated with Marcellus Shale gas development. *Water Resour. Res.* **2013**, *49*, 647−656. _eprint: https://agupubs.onlinelibrary.wiley.com/doi/pdf/10.1002/wrcr.20096.

(31) Guarnone, M.; Rossi, F.; Negri, E.; Grassi, C.; Genazzi, D.; Zennaro, R. An unconventional mindset for shale gas surface facilities. *J. Nat. Gas Sci. Eng.* **2012**, *6*, 14−23.

(32) Ferrar, K. J.; Michanowicz, D. R.; Christen, C. L.; Mulcahy, N.; Malone, S. L.; Sharma, R. K. Assessment of Effluent Contaminants from Three Facilities Discharging Marcellus Shale Wastewater to Surface Waters in Pennsylvania. *Environ. Sci. Technol.* **2013**, *47*, 3472−3481.

(33) Menefee, A. H.; Ellis, B. R. Wastewater management strategies for sustained shale gas production. *Environ. Res. Lett.* **2020**, *15*, 024001.

(34) Coonrod, C. L.; ben Yin, Y.; Hanna, T.; Atkinson, A. J.; Alvarez, P. J. J.; Tekavec, T. N.; Reynolds, M. A.; Wong, M. S. Fit-for-purpose treatment goals for produced waters in shale oil and gas fields. *Water Res.* **2020**, *173*, 115467.

(35) Guerra, K.; Dahm, K.; Dundorf, S. *Oil and gas produced water management and beneficial use in the Western United States*; 2011.

(36) Liden, T.; Santos, I. C.; Hildenbrand, Z. L.; Schug, K. A. Treatment modalities for the reuse of produced waste from oil and gas development. *Sci. Total Environ.* **2018**, *643*, 107−118.

(37) Wenzlick, M.; Siefert, N. Techno-economic analysis of converting oil & gas produced water into valuable resources. *Desalination* **2020**, *481*, 114381.

(38) Tavakkoli, S.; Lokare, O.; Vidic, R.; Khanna, V. Shale gas produced water management using membrane distillation: An optimization-based approach. *Resources, Conservation and Recycling* **2020**, *158*, 104803.

(39) Benko, K. L.; Drewes, J. E. Produced Water in the Western United States: Geographical Distribution, Occurrence, and Composition. *Environ. Eng. Sci.* **2008**, *25*, 239−246.

(40) Barbot, E.; Vidic, N. S.; Gregory, K. B.; Vidic, R. D. Spatial and Temporal Correlation of Water Quality Parameters of Produced Waters from Devonian-Age Shale following Hydraulic Fracturing. *Environ. Sci. Technol.* **2013**, *47*, 2562−2569.

(41) Rosenblum, J.; Nelson, A. W.; Ruyle, B.; Schultz, M. K.; Ryan, J. N.; Linden, K. G. Temporal characterization of flowback and produced water quality from a hydraulically fractured oil and gas well. *Sci. Total Environ.* **2017**, *596*−*597*, 369−377.

(42) Hoelzer, K.; Sumner, A. J.; Karatum, O.; Nelson, R. K.; Drollette, B. D.; O'Connor, M. P.; D'Ambro, E. L.; Getzinger, G. J.; Ferguson, P. L.; Reddy, C. M.; Elsner, M.; Plata, D. L. Indications of Transformation Products from Hydraulic Fracturing Additives in Shale-Gas Wastewater. *Environ. Sci. Technol.* **2016**, *50*, 8036−8048.

(43) Lester, Y.; Ferrer, I.; Thurman, E. M.; Sitterley, K. A.; Korak, J. A.; Aiken, G.; Linden, K. G. Characterization of hydraulic fracturing flowback water in Colorado: Implications for water treatment. *Sci. Total Environ.* **2015**, *512*−*513*, 637−644.
(44) Rosenblum, J.; Thurman, E. M.; Ferrer, I.; Aiken, G.; Linden, K. G. Organic Chemical Characterization and Mass Balance of a Hydraulically Fractured Well: From Fracturing Fluid to Produced Water over 405 Days. *Environ. Sci. Technol.* **2017**, *51*, 14006−14015.
(45) Paukert Vankeuren, A. N.; Hakala, J. A.; Jarvis, K.; Moore, J. E. Mineral Reactions in Shale Gas Reservoirs: Barite Scale Formation from Reusing Produced Water As Hydraulic Fracturing Fluid. *Environ. Sci. Technol.* **2017**, *51*, 9391−9402.
(46) Russell, T.; Pham, D.; Neishaboor, M. T.; Badalyan, A.; Behr, A.; Genolet, L.; Kowollik, P.; Zeinijahromi, A.; Bedrikovetsky, P. Effects of kaolinite in rocks on fines migration. *J. Nat. Gas Sci. Eng.* **2017**, *45*, 243−255.
(47) Gale, J. F. W.; Laubach, S. E.; Olson, J. E.; Eichhubl, P.; Fall, A. Natural fractures in shale: A review and new observations. *AAPG Bull.* **2014**, *98*, 2165−2216.
(48) Barati, R.; Liang, J.-T. A review of fracturing fluid systems used for hydraulic fracturing of oil and gas wells. *J. Appl. Polym. Sci.* 2014, *131*, _eprint: https://onlinelibrary.wiley.com/doi/pdf/10.1002/app.40735.
(49) Gensterblum, Y.; Ghanizadeh, A.; Cuss, R. J.; Amann-Hildenbrand, A.; Krooss, B. M.; Clarkson, C. R.; Harrington, J. F.; Zoback, M. D. Gas transport and storage capacity in shale gas reservoirs − A review. Part A: Transport processes. *Journal of Unconventional Oil and Gas Resources* **2015**, *12*, 87−122.
(50) Xu, C.; Kang, Y.; You, Z.; Chen, M. Review on formation damage mechanisms and processes in shale gas reservoir: Known and to be known. *J. Nat. Gas Sci. Eng.* **2016**, *36*, 1208−1219.
(51) Siddiqui, M. A. Q.; Ali, S.; Fei, H.; Roshan, H. Current understanding of shale wettability: A review on contact angle measurements. *Earth-Sci. Rev.* **2018**, *181*, 1−11.
(52) Békri, S.; Thovert, J. F.; Adler, P. M. Dissolution of porous media. *Chem. Eng. Sci.* **1995**, *50*, 2765−2791.
(53) Alemu, B. L.; Aagaard, P.; Munz, I. A.; Skurtveit, E. Caprock interaction with CO2: A laboratory study of reactivity of shale with supercritical CO2 and brine. *Appl. Geochem.* **2011**, *26*, 1975−1989.
(54) Wu, W.; Sharma, M. M. Acid Fracturing in Shales: Effect of Dilute Acid on Properties and Pore Structure of Shale. *SPE Production & Operations* **2017**, *32*, 51−63.
(55) Shovkun, I.; Espinoza, D. Nicolas, Shale Acid Fracturing: Geomechanical Effects and Fracture Propagation. *Poromechanics VI* **2017**, 1924−1929.
(56) Jew, A. D.; Li, Q.; Cercone, D.; Maher, K.; Brown, G. E. J.; Bargar, J. R. *Barium Sources in Hydraulic Fracturing Systems and Chemical Controls on Its Release Into Solution*. 2018.
(57) Alalli, A. A.; Li, Q.; Jew, A.; Kohli, A.; Bargar, J.; Zoback, M.; Kovscek, A. Effects of Hydraulic Fracturing Fluid Chemistry on Shale Matrix Permeability; *Unconventional Resources Technology Conference (URTEC)*, 2018.
(58) Pournik, M.; Tripathi, D.; Monier, I. E. Productivity of Hydraulically Fractured Calcite Rich Shale Reservoirs Enhanced by Acid. *Journal of Petroleum Engineering & Technology* **2019**, *6* (1), 54−68.
(59) Li, Q.; Jew, A. D.; Brown, G. E.; Bargar, J. R.; Maher, K. Reactive Transport Modeling of Shale−Fluid Interactions after Imbibition of Fracturing Fluids. *Energy Fuels* 2020.
(60) Alsaba, M.; Al Marshad, A.; Abbas, A.; Abdulkareem, T.; Al-Shammary, A.; Al-Ajmi, M.; Kebeish, E. Laboratory evaluation to assess the effectiveness of inhibitive nano-water-based drilling fluids for Zubair shale formation. *J. Pet. Explor. Prod. Technol.* **2020**, *10*, 419−428.
(61) Ilgen, A. G.; Mook, W. M.; Tigges, A. B.; Choens, R. C.; Artyushkova, K.; Jungjohann, K. L. Chemical controls on the propagation rate of fracture in calcite. *Sci. Rep.* **2018**, *8*, 16465. Number: 1 Publisher: Nature Publishing Group.
(62) Zhao, X.; He, E.; Guo, J.; Zhu, H.; Wang, H.; He, W. The study of fracture propagation in pre-acidized shale reservoir during the hydraulic fracturing. *J. Pet. Sci. Eng.* **2020**, *184*, 106488.
(63) Frampton, A.; Hyman, J. D.; Zou, L. Advective Transport in Discrete Fracture Networks With Connected and Disconnected Textures Representing Internal Aperture Variability. *Water Resour. Res.* **2019**, *55*, 5487−5501. _eprint: https://agupubs.onlinelibrary.wiley.com/doi/pdf/10.1029/2018WR024322.
(64) Osiptsov, A. A. Fluid Mechanics of Hydraulic Fracturing: a Review. *J. Pet. Sci. Eng.* **2017**, *156*, 513−535.
(65) Karra, S.; Makedonska, N.; Viswanathan, H. S.; Painter, S. L.; Hyman, J. D. Effect of advective flow in fractures and matrix diffusion on natural gas production. *Water Resour. Res.* **2015**, *51*, 8646−8657. Publisher: John Wiley & Sons, Ltd.
(66) Makedonska, N.; Karra, S.; Viswanathan, H. S.; Guthrie, G. D. Role of Interaction between Hydraulic and Natural Fractures on Production. *J. Nat. Gas Sci. Eng.* **2020**, *82*, 103451.
(67) Tokunaga, T. K.; Shen, W.; Wan, J.; Kim, Y.; Cihan, A.; Zhang, Y.; Finsterle, S. Water Saturation Relations and Their Diffusion-Limited Equilibration in Gas Shale: Implications for Gas Flow in Unconventional Reservoirs. *Water Resour. Res.* **2017**, *53*, 9757−9770. _eprint: https://agupubs.onlinelibrary.wiley.com/doi/pdf/10.1002/2017WR021153.
(68) Javadpour, F. Nanopores and Apparent Permeability of Gas Flow in Mudrocks (Shales and Siltstone). *Journal of Canadian Petroleum Technology* **2009**, *48*, 16−21.
(69) Lee, K. S.; Kim, T. H. In *Transport in Shale Reservoirs*. Lee, K. S., Kim, T. H., Eds.; Gulf Professional Publishing, 2019; pp 35−67.
(70) Kenomore, M.; Hassan, M.; Malakooti, R.; Dhakal, H.; Shah, A. Shale gas production decline trend over time in the Barnett Shale. *J. Pet. Sci. Eng.* **2018**, *165*, 691−710.
(71) Mengal, S. A.; Wattenbarger, R. A. *Accounting For Adsorbed Gas in Shale Gas Reservoirs*. 2011.
(72) Wang, H. *What Factors Control Shale Gas Production Decline Trend: A Comprehensive Analysis and Investigation*. **2016**. DOI: 10.2118/179967-MS
(73) Xu, J.; Ding, Y.; Yang, L.; Liu, Z.; Gao, R.; Yang, H.; Wang, Z. Effect of proppant deformation and embedment on fracture conductivity after fracturing fluid loss. *J. Nat. Gas Sci. Eng.* **2019**, *71*, 102986.
(74) Balashov, V. N.; Guthrie, G. D.; Lopano, C. L.; Hakala, J. A.; Brantley, S. L. Reaction and diffusion at the reservoir/shale interface during CO2 storage: Impact of geochemical kinetics. *Appl. Geochem.* **2015**, *61*, 119−131.
(75) Lovell, A. E.; Srinivasan, S.; Karra, S.; O'Malley, D.; Makedonska, N.; Viswanathan, H. S.; Srinivasan, G.; Carey, J. W.; Frash, L. P. Extracting Hydrocarbon From Shale: An Investigation of the Factors That Influence the Decline and the Tail of the Production Curve. *Water Resour. Res.* **2018**, *54*, 3748−3757. _eprint: https://agupubs.onlinelibrary.wiley.com/doi/pdf/10.1029/2017WR022180.
(76) Lee, K. S.; Kim, T. H. In *Transport in Shale Reservoirs*. Lee, K. S., Kim, T. H., Eds.; Gulf Professional Publishing, 2019; pp 7−34.
(77) Wang, G.; Carr, T. R. Organic-rich Marcellus Shale lithofacies modeling and distribution pattern analysis in the Appalachian BasinOrganic-Rich Shale Lithofacies Modeling, Appalachian Basin. *AAPG Bull.* **2013**, *97*, 2173−2205.
(78) Sone, H.; Zoback, M. D. Mechanical properties of shale-gas reservoir rocks - Part 1: Static and dynamic elastic properties and anisotropy. *Geophysics* **2013**, *78*, D381−D392.
(79) Shoemaker, M.; Zakhour, N.; Peacock, J. *Integrating 3D Seismic and Geomechanical Properties with Microseismic Acquisition and Fracturing Parameters to Optimize Completion Practices within the Wolfcamp Shale Play of the Midland Basin*. **2015**. DOI: 10.2118/178575-MS
(80) Adesida, A. G.; Akkutlu, I.; Resasco, D. E.; Rai, C. S. *Characterization of Barnett Shale Kerogen Pore Size Distribution using DFT Analysis and Grand Canonical Monte Carlo Simulations*. **2011**. DOI: 10.2118/147397-MS

(81) Ilgen, A. G.; Heath, J. E.; Akkutlu, I. Y.; Bryndzia, L. T.; Cole, D. R.; Kharaka, Y. K.; Kneafsey, T. J.; Milliken, K. L.; Pyrak-Nolte, L. J.; Suarez-Rivera, R. Shales at all scales: Exploring coupled processes in mudrocks. *Earth-Sci. Rev.* **2017**, *166*, 132−152.
(82) Schieber, J.; Lazar, R.; Bohacs, K.; Klimentidis, R.; Dumitrescu, M.; Ottmann, J. In *The Eagle Ford Shale: A renaissance in U.S. oil production*. Breyer, J. A., Ed.; AAPG Memoir 110; American Association of Petroleum Geologists Special Volumes, 2016; pp 167−186.
(83) Frouté, L.; Kovscek, A. R. Nano-Imaging of Shale Using Electron Microscopy Techniques; *Proceedings of the Unconventional Resources Technology Conference (URTeC)*. Virtual, 2020.
(84) Walsh, J. B.; Brace, W. F. The effect of pressure on porosity and the transport properties of rock. *J. Geophys. Res.* **1984**, *89*, 9425−9431.
(85) Ougier-Simonin, A.; Renard, F.; Boehm, C.; Vidal-Gilbert, S. Microfracturing and microporosity in shales. *Earth-Sci. Rev.* **2016**, *162*, 198−226.
(86) Aljamaan, H.; Ross, C. M.; Kovscek, A. R. Multiscale Imaging of Gas Storage in Shales. *SPE Journal* **2017**, *22*, 1760−1777.
(87) Saraji, S.; Piri, M. The representative sample size in shale oil rocks and nano-scale characterization of transport properties. *Int. J. Coal Geol.* **2015**, *146*, 42−54.
(88) Jarvie, D. M. *Shale Resource Systems for Oil and Gas: Part 2−Shale-oil Resource Systems* **2012**, 89−119.
(89) Wang, S.; Feng, Q.; Javadpour, F.; Xia, T.; Li, Z. Oil adsorption in shale nanopores and its effect on recoverable oil-in-place. *Int. J. Coal Geol.* **2015**, *147−148*, 9−24.
(90) Andrew, M. Vaca Muerta FIB-SEM. 2019; http://www.digitalrocksportal.org/projects/207.
(91) Bowker, K. A. Recent developments of the Barnett Shale play, Fort Worth basin. *West Texas Geological Society Bulletin* **2003**, *42*, 4−11.
(92) Givens, N.; Zhao, H. The Barnett Shale: Not so simple after all (abs.): AAPG Annual Meeting Program, v. 13, p. *A52* 2004.
(93) Loucks, R. G.; Ruppel, S. C. Mississippian Barnett Shale: Lithofacies and depositional setting of a deep-water shale-gas succession in the Fort Worth Basin, Texas. *AAPG Bull.* **2007**, *91*, 579−601.
(94) Paktinat, J.; Pinkhouse, J. A.; Little, J. B.; Lash, G. G.; Penny, G. S. *Investigation of Methods to Improve Utica Shale Hydraulic Fracturing in the Appalachian Basin*. **2007**. DOI: 10.2118/111063-MS
(95) Jarvie, D. M.; Hill, R. J.; Ruble, T. E.; Pollastro, R. M. Unconventional shale-gas systems: The Mississippian Barnett Shale of north-central Texas as one model for thermogenic shale-gas assessment. *AAPG Bull.* **2007**, *91*, 475−499.
(96) Bruner, K.; Smosna, R. *A comparative study of the Mississippian Barnett Shale, Fort Worth Basin, and Devonian Marcellus Shale, Appalachian Basin*. Report to US Dept. of Energy (US DOE). National Technology Laboratory. *Energy Technology Laboratory DOE/NETL-2011/1478. URS Corporation (April, 108 pp.)*. 2011.
(97) Harris, N. B.; Miskimins, J. L.; Mnich, C. A. Mechanical anisotropy in the Woodford Shale, Permian Basin: Origin, magnitude, and scale. *Leading Edge* **2011**, *30*, 284−291.
(98) Deville, J. P.; Fritz, B.; Jarrett, M. Development of Water-Based Drilling Fluids Customized for Shale Reservoirs. *SPE Drilling & Completion* **2011**, *26*, 484−491.
(99) Ratcliffe, K.; Wright, A.; Schmidt, K. Application of inorganic whole-rock geochemistry to shale resource plays: an example from the Eagle Ford Shale Formation, Texas. *Sedimentary Record* **2012**, *10*, 4−9.
(100) Bernard, S.; Wirth, R.; Schreiber, A.; Schulz, H.-M.; Horsfield, B. Formation of nanoporous pyrobitumen residues during maturation of the Barnett Shale (Fort Worth Basin). *Int. J. Coal Geol.* **2012**, *103*, 3−11.
(101) Chalmers, G. R.; Bustin, R. M.; Power, I. M. Characterization of gas shale pore systems by porosimetry, pycnometry, surface area, and field emission scanning electron microscopy/transmission electron microscopy image analyses: Examples from the Barnett, Woodford, Haynesville, Marcellus, and Doig unitsCharacterization of Gas Shale Pore Systems. *AAPG Bull.* **2012**, *96*, 1099−1119.
(102) Gupta, N.; Rai, C. S.; Sondergeld, C. H. *Integrated Petrophysical Characterization of the Woodford Shale In Oklahoma*. **2012**.
(103) Ali, M.; Hascakir, B. *Water-Rock Interaction for Eagle Ford, Marcellus, Green River, and Barnett Shale Samples*. **2015**. DOI: 10.2118/177304-MS
(104) Frash, L. P.; Carey, J. W.; Lei, Z.; Rougier, E.; Ickes, T.; Viswanathan, H. S. High-stress triaxial direct-shear fracturing of Utica shale and in situ X-ray microtomography with permeability measurement. *Journal of Geophysical Research: Solid Earth* **2016**, *121*, 5493−5508. _eprint: https://agupubs.onlinelibrary.wiley.com/doi/pdf/10.1002/2016JB012850.
(105) Al Ismail, M. I.; Zoback, M. D. Effects of rock mineralogy and pore structure on stress-dependent permeability of shale samples. *Philos. Trans. R. Soc., A* **2016**, *374*, 20150428. Publisher: Royal Society.
(106) Marcon, V.; Joseph, C.; Carter, K. E.; Hedges, S. W.; Lopano, C. L.; Guthrie, G. D.; Hakala, J. A. Experimental insights into geochemical changes in hydraulically fractured Marcellus Shale. *Appl. Geochem.* **2017**, *76*, 36−50.
(107) Jew, A. D.; Dustin, M. K.; Harrison, A. L.; Joe-Wong, C. M.; Thomas, D. L.; Maher, K.; Brown, G. E.; Bargar, J. R. Impact of Organics and Carbonates on the Oxidation and Precipitation of Iron during Hydraulic Fracturing of Shale. *Energy Fuels* **2017**, *31*, 3643−3658.
(108) Ko, L. T.; Loucks, R. G.; Ruppel, S. C.; Zhang, T.; Peng, S. Origin and characterization of Eagle Ford pore networks in the south Texas Upper Cretaceous shelf. *AAPG Bull.* **2017**, *101*, 387−418.
(109) Li, Q.; Jew, A. D.; Kiss, A. M.; Kohli, A.; Alalli, A.; Kovscek, A. R.; Zoback, M. D.; Cercone, D.; Maher, K.; Brown, G. E.; Bargar, J. R. *Imaging Pyrite Oxidation and Barite Precipitation in Gas and Oil Shales* Houston, TX, 2018; pp 875−884.
(110) Farrokhpay, S.; Ndlovu, B.; Bradshaw, D. Behaviour of swelling clays versus non-swelling clays in flotation. *Miner. Eng.* **2016**, *96−97*, 59−66.
(111) Stephen, I.; MacEwan, D. M. C. Swelling Chlorite. *Geotechnique* **1950**, *2*, 82−83.
(112) Chenevert, M. E. Shale Alteration by Water Adsorption. *JPT, J. Pet. Technol.* **1970**, *22*, 1141−1148.
(113) Madsen, F. T.; Müller-Vonmoos, M. The swelling behaviour of clays. *Appl. Clay Sci.* **1989**, *4*, 143−156.
(114) Laird, D. A. Influence of layer charge on swelling of smectites. *Appl. Clay Sci.* **2006**, *34*, 74−87.
(115) Chalmers, G. R. L.; Bustin, R. M. A multidisciplinary approach in determining the maceral (kerogen type) and mineralogical composition of Upper Cretaceous Eagle Ford Formation: Impact on pore development and pore size distribution. *Int. J. Coal Geol.* **2017**, *171*, 93−110.
(116) Wilson, M. J.; Shaldybin, M. V.; Wilson, L. Clay mineralogy and unconventional hydrocarbon shale reservoirs in the USA. I. Occurrence and interpretation of mixed-layer R3 ordered Illite/smectite. *Earth-Sci. Rev.* **2016**, *158*, 31−50.
(117) Montgomery, S. L.; Jarvie, D. M.; Bowker, K. A.; Pollastro, R. M. Mississippian Barnett Shale, Fort Worth basin, north-central Texas: Gas-shale play with multi−trillion cubic foot potential. *AAPG Bull.* **2005**, *89*, 155−175.
(118) Engelder, T.; Lash, G. G.; Uzcátegui, R. S. Joint sets that enhance production from Middle and Upper Devonian gas shales of the Appalachian Basin. *AAPG Bull.* **2009**, *93*, 857−889.
(119) Luo, J.; Ramos, M.; Espinoza, D. N. *Fracture Patterns in Laminated Mancos Shale*; Digital Rocks Portal, 2019.
(120) Gale, J. F. W.; Holder, J. *Natural fractures in the Barnett Shale: constraints on spatial organization and tensile strength with implications for hydraulic fracture treatment in shale-gas reservoirs*. 2008.
(121) Ground Water Protection Council, *Modern shale gas development in the United States: A primer*; 2009.

(122) Rao, V.; Knight, R. In *Sustainable Shale Oil and Gas*. Rao, V., Knight, R., Eds.; Elsevier, 2017; pp 75−91.
(123) Kaufman, P. B.; Penny, G. S.; Paktinat, J. *Critical Evaluation of Additives Used in Shale Slickwater Fracs*. **2008**. DOI: 10.2118/119900-MS
(124) Burden, S.; Fleming, M.; Frithsen, J.; Hills, L.; Klewicki, K.; Knightes, C. et al. *Hydraulic fracturing for oil and gas: Impacts from the hydraulic fracturing water cycle on drinking water resources in the United States*; US EPA: Washington, DC, 2016.
(125) Mirakyan, A.; Brown, D.; Sethi, R.; Mcmahon, B.; Mackay, B.; Perroni, D. *Low molecular weight guar as gelling agent additive*. Library Catalog: Google Patents 2017.
(126) Nasr-El-Din, H. A.; Al-Mohammed, A. M.; Al-Aamri, A. D.; Al-Fuwaires, O. A. *A Study of Gel Degradation, Surface Tension, and Their Impact on the Productivity of Hydraulically Fractured Gas Wells*. **2007**. DOI: 10.2523/IPTC-11585-MS
(127) Li, L.; Al-Muntasheri, G. A.; Liang, F. A review of crosslinked fracturing fluids prepared with produced water. *Petroleum* **2016**, *2*, 313−323.
(128) Sarwar, M. U. *Degradation of Guar-Based Fracturing Gels: A Study of Oxidative and Enzymatic Breakers* Thesis, 2010; Accepted: 2012−02−14T22:19:08Z.
(129) Liang, F.; Sayed, M.; Al-Muntasheri, G. A.; Chang, F. F.; Li, L. A comprehensive review on proppant technologies. *Petroleum* **2016**, *2*, 26−39.
(130) Ba Geri, M.; Imqam, A.; Flori, R. *A Critical Review of Using High Viscosity Friction Reducers as Fracturing Fluids for Hydraulic Fracturing Applications*. **2019**. DOI: 10.2118/195191-MS
(131) Dustin, M. K.; Bargar, J. R.; Jew, A. D.; Harrison, A. L.; Joe-Wong, C.; Thomas, D. L.; Brown, G. E.; Maher, K. Shale Kerogen: Hydraulic Fracturing Fluid Interactions and Contaminant Release. *Energy Fuels* **2018**, *32*, 8966−8977. Publisher: American Chemical Society.
(132) Crowe, C.; McConnell, S. B.; Hinkel, J. J.; Chapman, K. *Scale Inhibition in Wellbores*. **1994**. DOI: 10.2118/27996-MS
(133) Fan, C.; Kan, A. T.; Zhang, P.; Lu, H.; Work, S.; Yu, J.; Tomson, M. B. *Scale prediction and inhibition for unconventional oil and gas production*. **2010**. DOI: 10.2118/130690-MS
(134) Kahrilas, G. A.; Blotevogel, J.; Stewart, P. S.; Borch, T. Biocides in Hydraulic Fracturing Fluids: A Critical Review of Their Usage, Mobility, Degradation, and Toxicity. *Environ. Sci. Technol.* **2015**, *49*, 16−32.
(135) Kefi, S.; Lee, J.; Pope, T.; Sullivan, P.; Nelson, E.; Hernandez, A.; Olsen, T.; Parlar, M.; Powers, B.; Roy, A.; et al. Expanding applications for viscoelastic surfactants. *Oilfield Review* **2004**, *16*, 10−23.
(136) Zhou, L.; Das, S.; Ellis, B. R. Effect of Surfactant Adsorption on the Wettability Alteration of Gas-Bearing Shales. *Environ. Eng. Sci.* **2016**, *33*, 766−777.
(137) Montgomery, C. *Fracturing Fluids*. **2013**. DOI: 10.5772/56192
(138) Maley, D.; Farion, G.; Giurea-Bica, G.; O'Neil, B. *Non-Polymeric Permanent Clay Stabilizer for Shale Completions*. **2013**. DOI: 10.2118/165168-MS
(139) Steudel, A.; Batenburg, L. F.; Fischer, H. R.; Weidler, P. G.; Emmerich, K. Alteration of swelling clay minerals by acid activation. *Appl. Clay Sci.* **2009**, *44*, 105−115.
(140) Steudel, A.; Batenburg, L. F.; Fischer, H. R.; Weidler, P. G.; Emmerich, K. Alteration of non-swelling clay minerals and magadiite by acid activation. *Appl. Clay Sci.* **2009**, *44*, 95−104.
(141) Wang, L.; Fortner, J. D.; Giammar, D. E. Impact of Water Chemistry on Element Mobilization from Eagle Ford Shale. *Environ. Eng. Sci.* **2015**, *32*, 310−320.
(142) Harrison, A. L.; Jew, A. D.; Dustin, M. K.; Thomas, D. L.; Joe-Wong, C. M.; Bargar, J. R.; Johnson, N.; Brown, G. E.; Maher, K. Element release and reaction-induced porosity alteration during shale-hydraulic fracturing fluid interactions. *Appl. Geochem.* **2017**, *82*, 47−62.
(143) Alohaly, M.; BinGhanim, A.; Rahal, R.; Rahim, S. *Seawater Fracturing Fluid Development Challenges: A Comparison Between Seawater-Based and Freshwater-Based Fracturing Fluids Using Two Types of Guar Gum Polymers*. **2016**. DOI: 10.2118/182799-MS
(144) Chilkoor, G.; Shrestha, N.; Soeder, D.; Gadhamshetty, V. Corrosion and environmental impacts during the flowback water disposal associated with the Bakken shale. *Corros. Sci.* **2018**, *133*, 48−60.
(145) Wickard, A. K.; Elmore, R. D.; Heij, G. *A Diagenetic Study of the Wolfcamp Shale, Midland Basin, West Texas*. **2016**. DOI: 10.15530/urtec-2016-2460784
(146) He, C.; Li, M.; Liu, W.; Barbot, E.; Vidic, R. D. Kinetics and Equilibrium of Barium and Strontium Sulfate Formation in Marcellus Shale Flowback Water. *J. Environ. Eng.* **2014**, *140*, B4014001.
(147) Mouser, P. J.; Borton, M.; Darrah, T. H.; Hartsock, A.; Wrighton, K. C. Hydraulic fracturing offers view of microbial life in the deep terrestrial subsurface. *FEMS Microbiology Ecology*; Oxford Academic, 2016, Vol. *92*.
(148) Liang, R.; Davidova, I. A.; Marks, C. R.; Stamps, B. W.; Harriman, B. H.; Stevenson, B. S.; Duncan, K. E.; Suflita, J. M. Metabolic Capability of a Predominant Halanaerobium sp. in Hydraulically Fractured Gas Wells and Its Implication in Pipeline Corrosion. *Front. Microbiol.* **2016**, *7*, 7.
(149) Cluff, M. A.; Hartsock, A.; MacRae, J. D.; Carter, K.; Mouser, P. J. Temporal Changes in Microbial Ecology and Geochemistry in Produced Water from Hydraulically Fractured Marcellus Shale Gas Wells. *Environ. Sci. Technol.* **2014**, *48*, 6508−6517.
(150) Bottero, S.; Picioreanu, C.; Enzien, M. V.; Van Loosdrecht, M.; Bruining, J.; Heimovaara, T. *Formation Damage and Impact on Gas Flow Caused by Biofilms Growing Within Proppant Packing Used in Hydraulic Fracturing*. **2010**. DOI: 10.2118/128066-MS
(151) Prandel, L. V.; Dias, N. M. P.; da Costa Saab, S.; Brinatti, A. M.; Giarola, N. F. B.; Pires, L. F. Characterization of kaolinite in the hardsetting clay fraction using atomic force microscopy, X-ray diffraction, and the Rietveld method. *J. Soils Sediments* **2017**, *17*, 2144−2155.
(152) Wang, Q.; Zhu, C.; Yun, J.; Yang, G. Isomorphic Substitutions in Clay Materials and Adsorption of Metal Ions onto External Surfaces: A DFT Investigation. *J. Phys. Chem. C* **2017**, *121*, 26722−26732.
(153) Liu, J.; Gaikwad, R.; Hande, A.; Das, S.; Thundat, T. Mapping and Quantifying Surface Charges on Clay Nanoparticles. *Langmuir* **2015**, *31*, 10469−10476.
(154) Schoonheydt, R. A.; Johnston, C. T. In *Developments in Clay Science*; Bergaya, F., Theng, B. K. G., Lagaly, G., Eds.; Handbook of Clay Science; Elsevier, 2006; Vol. *1* pp 87−113.
(155) Young, D. A.; Smith, D. E. Simulations of Clay Mineral Swelling and Hydration: Dependence upon Interlayer Ion Size and Charge. *J. Phys. Chem. B* **2000**, *104*, 9163−9170.
(156) Lagaly, G.; Ziesmer, S. Colloid chemistry of clay minerals: the coagulation of montmorillonite dispersions. *Adv. Colloid Interface Sci.* **2003**, *100−102*, 105−128.
(157) Chenevert, M. E. Shale Control with Balanced-Activity Oil-Continuous Muds. *JPT, J. Pet. Technol.* **1970**, *22*, 1309−1316.
(158) Lal, M. *Shale Stability: Drilling Fluid Interaction and Shale Strength*. **1999**. DOI: 10.2118/54356-MS
(159) Zhou, J. Interactions of organic-rich shale with water-based fluids. Thesis, 2015.
(160) Anderson, R. L.; Ratcliffe, I.; Greenwell, H. C.; Williams, P. A.; Cliffe, S.; Coveney, P. V. Clay swelling − A challenge in the oilfield. *Earth-Sci. Rev.* **2010**, *98*, 201−216.
(161) Luckham, P. F.; Rossi, S. The colloidal and rheological properties of bentonite suspensions. *Adv. Colloid Interface Sci.* **1999**, *82*, 43−92.
(162) Bishop, S. R. *Experimental Investigation of Formation Damage Due to the Induced Flocculation of Clays Within a Sandstone Pore Structure by a High Salinity Brine*. **1997**. DOI: 10.2118/38156-MS

(163) Gholami, R.; Elochukwu, H.; Fakhari, N.; Sarmadivaleh, M. A review on borehole instability in active shale formations: Interactions, mechanisms and inhibitors. *Earth-Sci. Rev.* **2018**, *177*, 2−13.
(164) Al-Arfaj, M. K.; Amanullah, M.; Sultan, A. S.; Hossain, M. E.; Abdulraheem, A. *Chemical and Mechanical Aspects of Wellbore Stability in Shale Formations: A Literature Review*. **2014**. DOI: 10.2118/171682-MS
(165) Chorom, M.; Rengasamy, P. Dispersion and zeta potential of pure clays as related to net particle charge under varying pH, electrolyte concentration and cation type. *Eur. J. Soil Sci.* **1995**, *46*, 657−665. _eprint: https://onlinelibrary.wiley.com/doi/pdf/10.1111/j.1365-2389.1995.tb01362.x.
(166) Nguyen, M. N.; Dultz, S.; Kasbohm, J.; Le, D. Clay dispersion and its relation to surface charge in a paddy soil of the Red River Delta, Vietnam. *J. Plant Nutr. Soil Sci.* **2009**, *172*, 477−486. _eprint: https://onlinelibrary.wiley.com/doi/pdf/10.1002/jpln.200700217.
(167) Wilson, M. J.; Wilson, L. Clay mineralogy and shale instability: an alternative conceptual analysis. *Clay Miner.* **2014**, *49*, 127−145.
(168) Tombácz, E.; Csanaky, C.; Illés, E. Polydisperse fractal aggregate formation in clay mineral and iron oxide suspensions, pH and ionic strength dependence. *Colloid Polym. Sci.* **2001**, *279*, 484−492.
(169) Aksu, I.; Bazilevskaya, E.; Karpyn, Z. T. Swelling of clay minerals in unconsolidated porous media and its impact on permeability. *GeoResJ.* **2015**, *7*, 1−13.
(170) Gulraiz, S.; Gray, K. E. Investigating the effects of plug viscosity on annular pressure drop and cuttings transport in a concentric annulus. *J. Nat. Gas Sci. Eng.* **2020**, *76*, 103210.
(171) Maurice, P. A.; Vierkorn, M. A.; Hersman, L. E.; Fulghum, J. E. Dissolution of well and poorly ordered kaolinites by an aerobic bacterium. *Chem. Geol.* **2001**, *180*, 81−97.
(172) Maurice, P. A.; Vierkorn, M. A.; Hersman, L. E.; Fulghum, J. E.; Ferryman, A. Enhancement of kaolinite dissolution by an aerobic Pseudomonas mendocina bacterium. *Geomicrobiol. J.* **2001**, *18*, 21−35.
(173) Mueller, B. Experimental Interactions Between Clay Minerals and Bacteria: A Review. *Pedosphere* **2015**, *25*, 799−810.
(174) Lagaly, G. In *Developments in Clay Science*; Bergaya, F., Theng, B. K. G., Lagaly, G., Eds.; Handbook of Clay Science; Elsevier, 2006; Vol. *1*; pp 141−245.
(175) Leong, Y. K. Charged patch attraction in dispersion: effect of polystyrene sulphonate molecular weight or patch size. *Colloid Polym. Sci.* **2001**, *279*, 82−87.
(176) Wilkinson, N.; Metaxas, A.; Ruud, E.; Raethke, E.; Wickramaratne, S.; Reineke, T. M.; Dutcher, C. S. Internal structure visualization of polymer − clay flocculants using fluorescence. *Colloid and Interface Science Communications* **2016**, *10*−*11*, 1−5.
(177) Wilkinson, N.; Metaxas, A.; Brichetto, E.; Wickramaratne, S.; Reineke, T. M.; Dutcher, C. S. Ionic strength dependence of aggregate size and morphology on polymer-clay flocculation. *Colloids Surf., A* **2017**, *529*, 1037−1046.
(178) Fu, L.; Liao, K.; Ge, J.; Huang, W.; Chen, L.; Sun, X.; Shifeng, zhang Study on the damage and control method of fracturing fluid to tight reservoir matrix. *J. Nat. Gas Sci. Eng.* **2020**, *82*, 103464.
(179) Lai, B.; Liang, F.; Zhang, J.; Li, L.; Liu, H.; Al-Muntasheri, G. *Fracturing Fluids Effects on Mechanical Properties of Organic Rich Shale*. **2016**.
(180) Gregory, K. B.; Vidic, R. D.; Dzombak, D. A. Water Management Challenges Associated with the Production of Shale Gas by Hydraulic Fracturing. *Elements* **2011**, *7*, 181−186.
(181) Yarushina, V. M.; Bercovici, D.; Oristaglio, M. L. Rock deformation models and fluid leak-off in hydraulic fracturing. *Geophys. J. Int.* **2013**, *194*, 1514−1526.
(182) Laughland, M. M.; Nelson, D. E.; Wilson, P.; Eastridge, E. *Uncharted Waters: What Can. We Learn From Waters Produced From Horizontal Wells in the Permian Basin?* Unconventional Resources Technology Conference (URTEC), 2014, .
(183) Dutta, R.; Lee, C.-H.; Odumabo, S.; Ye, P.; Walker, S. C.; Karpyn, Z. T.; Ayala H, L. F. Experimental Investigation of Fracturing-Fluid Migration Caused by Spontaneous Imbibition in Fractured Low-Permeability Sands. *SPE Reservoir Evaluation & Engineering* **2014**, *17*, 74−81.
(184) Liang, T.; Longoria, R. A.; Lu, J.; Nguyen, Q. P.; DiCarlo, D. A. *Enhancing Hydrocarbon Permeability After Hydraulic Fracturing: Laboratory Evaluations of Shut-ins and Surfactant Additives*. **2015**. DOI: 10.2118/175101-MS
(185) Zhou, Z.; Abass, H.; Li, X.; Bearinger, D.; Frank, W. Mechanisms of imbibition during hydraulic fracturing in shale formations. *J. Pet. Sci. Eng.* **2016**, *141*, 125−132.
(186) Civan, F. In *Reservoir Formation Damage*. Civan, F., Ed.; 3rd ed.; Gulf Professional Publishing: Boston, 2016; pp 9−30.
(187) Pedlow, J.; Sharma, M. *Changes in Shale Fracture Conductivity due to Interactions with Water-Based Fluids*. **2014**. DOI: 10.2118/168586-MS
(188) Guerra, J.; Zhu, D.; Hill, A. D. *Impairment of Fracture Conductivity in the Eagle Ford Shale Formation*. **2017**. DOI: 10.2118/184857-MS
(189) Du, J.; Hu, L.; Meegoda, J. N.; Zhang, G. Shale softening: Observations, phenomenological behavior, and mechanisms. *Appl. Clay Sci.* **2018**, *161*, 290−300.
(190) Wong, R. Swelling and softening behaviour of La Biche shale. *Can. Geotech. J.* **1998**, *35*, 206−221.
(191) Das, P.; Achalpurkar, M.; Pal, O. *Impact of Formation Softening and Rock Mechanical Properties on Selection of Shale Stimulation Fluid: Laboratory Evaluation*. **2014**. DOI: 10.2118/167787-MS
(192) van Oort, E.; Hale, A. H.; Mody, F. K.; Roy, S. Transport in Shales and the Design of Improved Water-Based Shale Drilling Fluids. *SPE Drilling & Completion* **1996**, *11*, 137−146.
(193) van Oort, E. *Physico-Chemical Stabilization of Shales*. **1997**. DOI: 10.2118/37263-MS
(194) Patel, A.; Stamatakis, S.; Young, S.; Friedheim, J. *Advances in Inhibitive Water-Based Drilling Fluids−Can. They Replace Oil-Based Muds?*. **2007**. DOI: 10.2118/106476-MS
(195) An, Y.; Yu, P. A strong inhibition of polyethyleneimine as shale inhibitor in drilling fluid. *J. Pet. Sci. Eng.* **2018**, *161*, 1−8.
(196) Zhang, J.; Zhu, D.; Hill, A. D. Water-Induced Damage to Propped-Fracture Conductivity in Shale Formations. *SPE Production & Operations* **2016**, *31*, 147−156.
(197) Berch, H. Predicting Potential Unconventional Production in the Tuscaloosa Marine Shale Play Using Thermal Modeling and Log Overlay Analysis. Ph.D. thesis, Louisiana State University and Agricultural and Mechanical College, 2013.
(198) Borrok, D. M.; Yang, W.; Wei, M.; Mokhtari, M. Heterogeneity of the mineralogy and organic content of the Tuscaloosa Marine Shale. *Mar. Pet. Geol.* **2019**, *109*, 717−731.
(199) Miller, Z. Multi-scale Nanoindentation for Characterization of Oil Shales. Ph.D. thesis, University of Mississippi, 2016.
(200) Pagels, M.; Willberg, D. M.; Edelman, E.; Zagorski, W.; Frantz, J. *Quantifying Fracturing Fluid Damage on Reservoir Rock to Optimize Production*. **2013**.1766
(201) Zhang, J.; Ouyang, L.; Zhu, D.; Hill, A. D. Experimental and numerical studies of reduced fracture conductivity due to proppant embedment in the shale reservoir. *J. Pet. Sci. Eng.* **2015**, *130*, 37−45.
(202) Zhang, K.; Kang, Y.; He, X.; Guo, Z.; Tian, G. Influence of proppant embedment on fracture conductivity. *IOP Conference Series: Earth and Environmental Science* **2020**, *446*, 052033.
(203) Newell, D. L.; Carey, J. W. Experimental Evaluation of Wellbore Integrity Along the Cement-rock Boundary. *Environ. Sci. Technol.* **2013**, *47*, 276−282.
(204) Noiriel, C.; Madé, B.; Gouze, P. Impact of coating development on the hydraulic and transport properties in argillaceous limestone fracture. *Water Resour. Res.* **2007**, *43*. DOI: 10.1029/2006WR005379
(205) Jew, A.; Harrison, A.; Dustin, M.; Joe-Wong, C.; Thomas, D.; Maher, K.; Brown, G.; Cercone, D.; Bargar, J. *Mineralogical and Porosity Alteration Following Fracture Fluid-Shale Reaction*; URTeC: Austin, TX, 2017.

(206) Lu, J.; Mickler, P. J.; Nicot, J.-P.; Choi, W.; Esch, W. L.; Darvari, R. Geochemical interactions of shale and brine in autoclave experiments—Understanding mineral reactions during hydraulic fracturing of Marcellus and Eagle Ford Shales. *AAPG Bull.* **2017**, *101*, 1567−1597.
(207) Palandri, J. L.; Kharaka, Y. K. *A compilation of rate parameters of water-mineral interaction kinetics for application to geochemical modeling*. **2004**. DOI: 10.3133/ofr20041068
(208) Morse, J. W.; Arvidson, R. S.; Lüttge, A. Calcium Carbonate Formation and Dissolution. *Chem. Rev.* **2007**, *107*, 342−381.
(209) Chen, Q.; You, L.; Kang, Y.; Dou, L.; Sheng, J. J. Gypsum-Crystallization-Induced Fracturing during Shale−Fluid Reactions and Application for Shale Stimulation. *Energy Fuels* **2018**, *32*, 10367−10381.
(210) Oetjen, K.; Chan, K. E.; Gulmark, K.; Christensen, J. H.; Blotevogel, J.; Borch, T.; Spear, J. R.; Cath, T. Y.; Higgins, C. P. Temporal characterization and statistical analysis of flowback and produced waters and their potential for reuse. *Sci. Total Environ.* **2018**, *619−620*, 654−664.
(211) Al-Roomi, Y. M.; Hussain, K. F. Potential kinetic model for scaling and scale inhibition mechanism. *Desalination* **2016**, *393*, 186−195.
(212) Li, J.; Tang, M.; Ye, Z.; Chen, L.; Zhou, Y. Scale formation and control in oil and gas fields: A review. *J. Dispersion Sci. Technol.* **2017**, *38*, 661−670.
(213) Hakala, J. A.; Crandall, D.; Moore, J.; Phan, T.; Sharma, S.; Lopano, C. *Laboratory-Scale Studies on Chemical Reactions Between Fracturing Fluid and Shale Core From the Marcellus Shale Energy and Environmental Laboratory (MSEEL) Site*. **2017**. DOI: 10.15530/urtec-2017-2670856
(214) Abouie, A.; Tagavifar, M.; Sanaei, A.; Sepehrnoori, K. *Production Loss by Scale Formation in Unconventional Reservoirs*. **2018**. DOI: 10.2118/190148-MS
(215) Osselin, F.; Saad, S.; Nightingale, M.; Hearn, G.; Desaulty, A.-M.; Gaucher, E. C.; Clarkson, C. R.; Kloppmann, W.; Mayer, B. Geochemical and sulfate isotopic evolution of flowback and produced waters reveals water-rock interactions following hydraulic fracturing of a tight hydrocarbon reservoir. *Sci. Total Environ.* **2019**, *687*, 1389−1400.
(216) Flynn, S.; Gunten, K. v.; Warchola, T.; Snihur, K.; Forbes, T. Z.; Goss, G. G.; Gingras, M. K.; Konhauser, K. O.; Alessi, D. S. Characterization and implications of solids associated with hydraulic fracturing flowback and produced water from the Duvernay Formation, Alberta, Canada. *Environmental Science: Processes & Impacts* **2019**, *21*, 242−255.
(217) Lauer, N. E.; Harkness, J. S.; Vengosh, A. Brine Spills Associated with Unconventional Oil Development in North Dakota. *Environ. Sci. Technol.* **2016**, *50*, 5389−5397.
(218) Renock, D.; Landis, J. D.; Sharma, M. Reductive weathering of black shale and release of barium during hydraulic fracturing. *Appl. Geochem.* **2016**, *65*, 73−86.
(219) Tieman, Z. G.; Stewart, B. W.; Capo, R. C.; Phan, T. T.; Lopano, C. L.; Hakala, J. A. Barium Isotopes Track the Source of Dissolved Solids in Produced Water from the Unconventional Marcellus Shale Gas Play. *Environ. Sci. Technol.* **2020**, *54*, 4275−4285.
(220) Menefee, A. H.; Welch, N. J.; Frash, L. P.; Hicks, W.; Carey, J. W.; Ellis, B. R. Rapid Mineral Precipitation During Shear Fracturing of Carbonate-Rich Shales. *J. Geophys. Res.: Solid Earth* **2020**, *125*, e2019JB018864. _eprint: https://agupubs.onlinelibrary.wiley.com/doi/pdf/10.1029/2019JB018864.
(221) Abualfaraj, N.; Gurian, P. L.; Olson, M. S. Characterization of Marcellus Shale Flowback Water. *Environ. Eng. Sci.* **2014**, *31*, 514−524.
(222) Zhang, P.; Liu, Y.; Zhang, N.; Kan, A. T.; Tomson, M. B. Experimental evaluation of attach-and-release mineral scale control strategy for aqueous fluid transporting pipelines. *Energy Fuels* 2019.
(223) Kan, A. T.; Fu, G.; Tomson, M. B. Effect of Methanol and Ethylene Glycol on Sulfates and Halite Scale Formation. *Ind. Eng. Chem. Res.* **2003**, *42*, 2399−2408. Publisher: American Chemical Society.
(224) Zhang, F.; Hinrichsen, C. J.; Kan, A. T.; Wang, W.; Wei, W.; Dai, Z.; Yan, F.; Liu, Y.; Bhandari, N.; Zhang, Z.; Ruan, G.; Tomson, M. B. Calcium Sulfate Scaling Risk and Inhibition for a Steamflood Project. *SPE Journal* **2017**, *22*, 881−891.
(225) He, S.; Kan, A. T.; Tomson, M. B. Mathematical Inhibitor Model for Barium Sulfate Scale Control. *Langmuir* **1996**, *12*, 1901−1905.
(226) Zhang, P.; Zhang, Z.; Zhu, J.; Kan, A. T.; Tomson, M. B. Experimental Evaluation of Common Sulfate Mineral Scale Coprecipitation Kinetics in Oilfield Operating Conditions. *Energy Fuels* **2019**, *33*, 6177−6186.
(227) Zhao, Y.; M. Sriyarathne, H. D.; Harouaka, K.; Paudyal, S.; Ko, S.; Dai, C.; Lu, A. Y.-T.; Deng, G.; Wang, X.; Kan, A. T.; Tomson, M. Evaluation of Silica Matrix Ion Effects on Barite Scale Inhibitors; *SPE International Conference on Oilfield Chemistry*, 8-9 April, Galveston, Texas, 2019.
(228) Zhang, Z.; Zhang, P.; Li, Z.; Kan, A. T.; Tomson, M. B. Laboratory Evaluation and Mechanistic Understanding of the Impact of Ferric Species on Oilfield Scale Inhibitor Performance. *Energy Fuels* **2018**, *32*, 8348−8357.
(229) Zhang, P.; Zhang, Z.; Liu, Y.; Kan, A. T.; Tomson, M. B. Investigation of the impact of ferrous species on the performance of common oilfield scale inhibitors for mineral scale control. *J. Pet. Sci. Eng.* **2019**, *172*, 288−296.
(230) Kan, A. T.; Dai, J. Z.; Deng, G.; Harouaka, K.; Lu, Y.-T.; Wang, X.; Zhao, Y.; Tomson, M. B. Recent Advances in Scale Prediction: Approach and Limitations. *SPE Journal* **2019**, *24*, 2209−2220.
(231) Yan, F.; Zhang, F.; Bhandari, N.; Wang, L.; Dai, Z.; Zhang, Z.; Liu, Y.; Ruan, G.; Kan, A.; Tomson, M. Adsorption and precipitation of scale inhibitors on shale formations. *J. Pet. Sci. Eng.* **2015**, *136*, 32−40.
(232) Zhang, L.; Kim, D.; Jun, Y.-S. The Effects of Phosphonate-Based Scale Inhibitor on Brine−Biotite Interactions under Subsurface Conditions. *Environ. Sci. Technol.* **2018**, *52*, 6042−6049.
(233) Mavredaki, E.; Neville, A.; Sorbie, K. S. Initial Stages of Barium Sulfate Formation at Surfaces in the Presence of Inhibitors. *Cryst. Growth Des.* **2011**, *11*, 4751−4758.
(234) He, C.; Vidic, R. D. Impact of Antiscalants on the Fate of Barite in the Unconventional Gas Wells. *Environ. Eng. Sci.* **2016**, *33*, 745−752.
(235) Herzig, J. P.; Leclerc, D. M.; Goff, P. L. Flow of Suspensions through Porous Media−Application to Deep Filtration. *Ind. Eng. Chem.* **1970**, *62*, 8−35.
(236) Gruesbeck, C.; Collins, R. E. Entrainment and Deposition of Fine Particles in Porous Media. *SPEJ, Soc. Pet. Eng. J.* **1982**, *22*, 847−856.
(237) Al-Abduwani, F. A. H. Internal filtration and external filter cake build-up in sandstones. Ph.D. thesis, TU Delft, Delft, Netherlands, 2005.
(238) Civan, F. *Reservoir Formation Damage*, 3rd ed.; Gulf Professional Publishing, 2015; p 1042.
(239) Khan, H. J.; Mirabolghasemi, M. S.; Yang, H.; Prodanović, M.; DiCarlo, D. A.; Balhoff, M. T. Study of formation damage caused by retention of bi-dispersed particles using combined pore-scale simulations and particle flooding experiments. *J. Pet. Sci. Eng.* **2017**, *158*, 293−308.
(240) Khilar, K. C.; Fogler, H. S. *Migrations of Fines in Porous Media*; Springer Science & Business Media, 1998.
(241) Mirabolghasemi, M.; Prodanović, M.; DiCarlo, D.; Ji, H. Prediction of empirical properties using direct pore-scale simulation of straining through 3D microtomography images of porous media. *J. Hydrol.* **2015**, *529*, 768−778.
(242) Khan, H. J.; DiCarlo, D.; Prodanović, M. The effect of vug distribution on particle straining in permeable media. *J. Hydrol.* **2020**, *580*, 124306.

(243) Khan, H. J.; Prodanovic, M.; DiCarlo, D. *Spatial and Temporal Patterns in Particle Retention in Vuggy Porous Media*. **2020**. DOI: 10.2118/199246-MS
(244) Wei, Y.; Li, C.; Cao, D.; Wang, A.; Zhang, A.; Yao, Z. The effects of particle size and inorganic mineral content on fines migration in fracturing proppant during coalbed methane production. *J. Pet. Sci. Eng.* **2019**, *182*, 106355.
(245) Kotlyar, L. S.; Sparks, B. D.; LePage, Y.; Woods, J. R. Effect of particle size on the flocculation behaviour of ultra-fine clays in salt solutions. *Clay Miner.* **1998**, *33*, 103−107.
(246) Rashid, M. A. *Geochemistry of Marine Humic Compounds*; Springer New York: New York, NY, 1985.
(247) Chang, H.; Li, T.; Liu, B.; Vidic, R. D.; Elimelech, M.; Crittenden, J. C. Potential and implemented membrane-based technologies for the treatment and reuse of flowback and produced water from shale gas and oil plays: A review. *Desalination* **2019**, *455*, 34−57.
(248) Haghshenas, A.; Nasr-El-Din, H. A. Effect of dissolved solids on reuse of produced water at high temperature in hydraulic fracturing jobs. *J. Nat. Gas Sci. Eng.* **2014**, *21*, 316−325.
(249) Padin, A.; Tutuncu, A. N.; Sonnenberg, S. *On the Mechanisms of Shale Microfracture Propagation*. **2014**. DOI: 10.2118/168624-MS
(250) Gale, J. F.; Elliott, S. J.; Laubach, S. E. Hydraulic Fractures in Core From Stimulated Reservoirs: Core Fracture Description of HFTS Slant Core, Midland Basin, West Texas; *Unconventional Resources Technology Conference*, Houston, Texas, 23−25 July 2018 2018; pp 1340−1357.
(251) Mahler, B. J.; Lynch, L.; Bennett, P. C. Mobile sediment in an urbanizing karst aquifer: implications for contaminant transport. *Environ. Geol.* **1999**, *39*, 25−38.
(252) Qajar, J.; Francois, N.; Arns, C. H. Microtomographic Characterization of Dissolution-Induced Local Porosity Changes Including Fines Migration in Carbonate Rock. *SPE Journal* **2013**, *18*, 545−562.
(253) Wu, W.; Zhou, J.; Kakkar, P.; Russell, R.; Sharma, M. M. An Experimental Study on Conductivity of Unpropped Fractures in Preserved Shales. *SPE Production & Operations* **2019**, *34*, 280−296.
(254) Schembre, J. M.; Kovscek, A. R. Mechanism of Formation Damage at Elevated Temperature. *J. Energy Resour. Technol.* **2005**, *127*, 171−180.
(255) Schembre, J. M.; Tang, G. Q.; Kovscek, A. R. Wettability alteration and oil recovery by water imbibition at elevated temperatures. *J. Pet. Sci. Eng.* **2006**, *52*, 131−148.
(256) Wu, W. Unpropped fractures in shale: surface topography, mechanical properties and hydraulic conductivity. Thesis, 2017.
(257) Ellis, B. R.; Fitts, J. P.; Bromhal, G. S.; McIntyre, D. L.; Tappero, R.; Peters, C. A. Dissolution-Driven Permeability Reduction of a Fractured Carbonate Caprock. *Environ. Eng. Sci.* **2013**, *30*, 187−193.
(258) Moore, R. L.; Loftin, D. F.; Palmer, I. D. *History Matching and Permeability Increases of Mature Coalbed Methane Wells in San Juan Basin*. **2011**. DOI: 10.2118/146931-MS
(259) Fredd, C. N.; McConnell, S. B.; Boney, C. L.; England, K. W. Experimental Study of Fracture Conductivity for Water-Fracturing and Conventional Fracturing Applications. *SPE Journal* **2001**, *6*, 288−298.
(260) Geri, M. B.; Flori, R.; Sherif, H. *Comprehensive Study of Elasticity and Shear-Viscosity Effects on Proppant Transport Using HFVRs on High-TDS Produced Water*. **2019**. DOI: 10.15530/urtec-2019-99
(261) Palisch, T. T.; Duenckel, R. J.; Chapman, M. A.; Woolfolk, S.; Vincent, M. C. *How to Use and Misuse Proppant Crush Tests − Exposing the Top 10 Myths*. **2009**. DOI: 10.2118/119242-MS
(262) Muecke, T. W. Formation Fines and Factors Controlling Their Movement in Porous Media. *JPT, J. Pet. Technol.* **1979**, *31*, 144−150.
(263) Gidley, J. L.; Penny, G. S.; McDaniel, R. R. Effect of Proppant Failure and Fines Migration on Conductivity of Propped Fractures. *SPE Prod. Facil.* **1995**, *10*, 20−25.
(264) Jia, Y.; Lu, Y.; Elsworth, D.; Fang, Y.; Tang, J. Surface characteristics and permeability enhancement of shale fractures due to water and supercritical carbon dioxide fracturing. *J. Pet. Sci. Eng.* **2018**, *165*, 284−297.
(265) Zhang, C. P.; Cheng, P.; Ranjith, P. G.; Lu, Y. Y.; Zhou, J. P. A comparative study of fracture surface roughness and flow characteristics between CO2 and water fracturing. *J. Nat. Gas Sci. Eng.* **2020**, *76*, 103188.
(266) Mighani, S.; Sondergeld, C. H.; Rai, C. S. Observations of Tensile Fracturing of Anisotropic Rocks. *SPE Journal* **2016**, *21*, 1,289−1,301.
(267) Sutherland, B. R.; Barrett, K. J.; Gingras, M. K. Clay settling in fresh and salt water. *Environ. Fluid Mech.* **2015**, *15*, 147−160.
(268) Żbik, M. S.; Frost, R. L. Micro-structure differences in kaolinite suspensions. *J. Colloid Interface Sci.* **2009**, *339*, 110−116.
(269) Borysenko, A.; Clennell, B.; Sedev, R.; Burgar, I.; Ralston, J.; Raven, M.; Dewhurst, D.; Liu, K. Experimental investigations of the wettability of clays and shales. *Journal of Geophysical Research: Solid Earth* _eprint: https://agupubs.onlinelibrary.wiley.com/doi/pdf/10.1029/2008JB005928 2009.
(270) Bai, B.; Elgmati, M.; Zhang, H.; Wei, M. Rock characterization of Fayetteville shale gas plays. *Fuel* **2013**, *105*, 645−652.
(271) Xu, M.; Dehghanpour, H. Advances in Understanding Wettability of Gas Shales. *Energy Fuels* **2014**, *28*, 4362−4375.
(272) Lan, Q.; Xu, M.; Binazadeh, M.; Dehghanpour, H.; Wood, J. M. A comparative investigation of shale wettability: The significance of pore connectivity. *J. Nat. Gas Sci. Eng.* **2015**, *27*, 1174−1188.
(273) Kathel, P.; Mohanty, K. K. Wettability Alteration in a Tight Oil Reservoir. *Energy Fuels* **2013**, *27*, 6460−6468.
(274) Alvarez, J. O.; Schechter, D. S. Wettability Alteration and Spontaneous Imbibition in Unconventional Liquid Reservoirs by Surfactant Additives. *SPE Reservoir Evaluation & Engineering* **2017**, *20*, 107−117. Publisher: Society of Petroleum Engineers.
(275) Elputranto, R.; Akkutlu, I. Y. *Near Fracture Capillary End Effect on Shale Gas and Water Production*; Unconventional Resources Technology Conference (URTEC), 2018.
(276) Shen, Y.; Ge, H.; Zhang, X.; Chang, L.; Liu, D.; Liu, J. Impact of fracturing liquid absorption on the production and water-block unlocking for shale gas reservoir. *Advances in Geo-Energy Research* **2018**, *2*, 163−172. Number: 2.
(277) Longoria, R. A.; Liang, T.; Huynh, U. T.; Nguyen, Q. P.; DiCarlo, D. A. Water Blocks in Tight Formations: The Role of Matrix/Fracture Interaction in Hydrocarbon-Permeability Reduction and Its Implications in the Use of Enhanced Oil Recovery Techniques. *SPE Journal* **2017**, *22*, 1,393−1,401.
(278) Liang, T.; Luo, X.; Nguyen, Q.; DiCarlo, D. A. Computed-Tomography Measurements of Water Block in Low-Permeability Rocks: Scaling and Remedying Production Impairment. *SPE Journal* **2018**, *23*, 762−771.
(279) Xie, Q.; Chen, Y.; You, L.; Hossain, M. M.; Saeedi, A. Drivers of Wettability Alteration for Oil/Brine/Kaolinite System: Implications for Hydraulic Fracturing Fluids Uptake in Shale Rocks. *Energies* **2018**, *11*, 1666. Number: 7 Publisher: Multidisciplinary Digital Publishing Institute.
(280) Al-Yaseri, A. Z.; Roshan, H.; Lebedev, M.; Barifcani, A.; Iglauer, S. Dependence of quartz wettability on fluid density. *Geophys. Res. Lett.* **2016**, *43*, 3771−3776. _eprint: https://agupubs.onlinelibrary.wiley.com/doi/pdf/10.1002/2016GL068278.
(281) Roshan, H.; Al-Yaseri, A. Z.; Sarmadivaleh, M.; Iglauer, S. On wettability of shale rocks. *J. Colloid Interface Sci.* **2016**, *475*, 104−111.